Pillars definition and dimensioning,
Verification and Validation of FEM parametric model

Arnaud Le Pivain

Master Thesis

presented in partial fulfillment
of the requirements for the double degree:
“Advanced Master in Naval Architecture” conferred by University of Liege
"Master of Sciences in Applied Mechanics, specialization in Hydrodynamics, Energetics and Propulsion” conferred by Ecole Centrale de Nantes

developed at West Pomeranian University of Technology, Szczecin
in the framework of the

“EMSHIP”
Erasmus Mundus Master Course
in “Integrated Advanced Ship Design”

Supervisor: Prof. Zbigniew Sekulski, West Pomeranian University of Technology, Szczecin

Reviewer: Prof. Kaeding P. , University of Rostock

Szczecin, February 2015

CONTENTS

TABLE OF FIGURES

TABLES

DECLARATION OF AUTHORSHIP

I declare that this thesis and the work presented in it are my own and have been generated by me as the result of my own original research.

Where I have consulted the published work of others, this is always clearly attributed.

Where I have quoted from the work of others, the source is always given. With the exception of such quotations, this thesis is entirely my own work.

I have acknowledged all main sources of help.

Where the thesis is based on work done by myself jointly with others, I have made clear exactly what was done by others and what I have contributed myself.

This thesis contains no material that has been submitted previously, in whole or in part, for the award of any other academic degree or diploma.

I cede copyright of the thesis in favour of West Pomeranian University of Technology, Szczecin

Date: 17/01/2015 *Signature:* 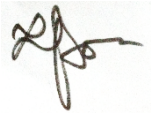

ABSTRACT

In the following master thesis, the author will describe the implementation of pillar staggering software based on an existing Excel sheet. The programming was made using VBA code. This software of thousands of code lines consists in two modes: one automatic and one manual.
The automatic one will provide a complete listing usable by the design office whereas the manual one will allow pillar and loading modification.

In a second time, a verification and validation process will be performed using solid FE model and laboratory analysis.

Special attention was given to the welds modeling and several FE model will be proposed.

The first model will be produced using an APDL macro in ANSYS mechanical. For this step, more than 1300 code lines were produced.

The additional models will be produced using ANSYS workbench. Particularly suitable for parametric modeling, this will allow to produce a solid parametric model for round and square pillar. These models will then be verified using laboratory tests and can then be used to validate the Excel sheet results.

At the end of this thesis, improvement proposals are made such as a global loop of optimization process.

This project was performed with the help of STX hull department using intern data.

This program was used on the Oasis 3 sister ship known at the date of the 1 January 2015 as the biggest passenger ship worldwide.

RESUMÉ

Dans le mémoire de master suivant, l'auteur s'attache à décrire la conception et la mise en œuvre d'un logiciel de calcul de décroissement d'épontilles. La programmation a été faite en utilisant le code VBA. Ce logiciel de plusieurs milliers de lignes de code autorise deux modes de calcul, l'un manuel, l'autre automatique.

Le mode automatique fournira une liste complète des décroissements d'épontilles. Cette liste de décroisement optimisé sera utilisable directement par le bureau d'études. La version manuelle permettra une modification au cas par cas des épontilles ou des chargements.

Dans un second temps, un processus de vérification et de validation sera effectué en utilisant un modèle EF solide et des tests fait en laboratoire.

Une attention particulière a été apportée à la modélisation des soudures dans le modèle FE.

Le premier modèle sera produit en utilisant une macro APDL avec ANSYS mécanique. Pour cette version, plus de 1300 lignes de code ont été produites.

Les modèles supplémentaires seront produits en utilisant ANSYS Workbench, particulièrement adapté pour la modélisation paramétrique. Cela permettra de produire un modèle paramétrique avec des éléments solides pour des profils d'épontilles rondes et carrées. Ces modèles seront ensuite vérifiés par comparaison avec les tests de laboratoire et pourront ensuite être utilisées pour valider les résultats de la feuille Excel.

A la fin de cette thèse, des propositions d'amélioration sont faites comme une boucle du processus d'optimisation sur le modèle global.

Ce projet a été réalisé avec l'aide du département calcul coque métallique de STX.

Ce programme de calcul a été utilisé sur le sister ship de l'Oasis 3 connu en date du 1 Janvier 2015 pour être le plus grand navire à passagers au monde.

ABBREVIATION

APDL: *ANSYS Parametric Design Language*

VBA: *Visual Basic for Applications*

FEM: *Finite Element Method*

FE: *Finite Element*

V&V: *Verification and Validation*

GA: *General Arrangement*

BV 2000: *Bureau Veritas 2000*

1. INTRODUCTION

This master thesis is about the definition and dimensioning of pillars using Visual Basic programming and verification & validation process by means of parametric solid Finite Element Model and laboratory tests.

In the context of fast shipbuilding, the design phase has to be as fast as possible. The structure calculation must be quickly done to give more time to the designers to propose new building options to the customer and to be reactive regarding the production process. The weight is a constant concern for designers. So optimization of each standard part could eventually lead to a huge gain of weight. In the case of pillars, sometimes more than 3000 of them are presented onboard. Few kilos gained on each pillar could conduct to a total mass gain that could be interesting. Of course this will remain small compared to the global ship weight but if this gain is made in each structure's component it could quickly become not negligible. A financial gain in the material could then directly be expected.

This gain could only occur using accurate calculations and good monitoring of the constraints.

The aim of this project is to study the different types of pillars staggering and especially to design a simple piece of software to optimize the pillars reinforcements. The work produced is a tool helping designers to make the right pillars and reinforcements (platting and welding) choice according to a predefined loading. This choice is made based on analytical calculation that includes FEM results and will be validated using local solid FE model and experimental analysis previously done.

The first task was to perform a friendly user, clear and simple tools that produce a database to provide to the design office.

The work was based on an existing excel sheet from the hull department calculating reinforcement for one single pillar. The new tool allows more flexibility and provides a listing of the reinforcement to be produce for several pillars at one time. The method used for computation includes flexion by using the moment of inertia of the section at different level in the reinforcement.

Pillars staggering for all kind of vessel could be consider with this program. As said in the appendixes, it was used on the *Oasis 3* sister ship known as the biggest passenger ship on the date of the first of January 2015.

As we will see later more in details, as an input, this software will take geometry and loading condition and the output will be an optimize reinforcement with the stresses and moment for each pillar junction listed according to its position. Two software versions are available, one manual that allow pillar geometry modification and one automatic that should be used on the global ship as it is producing a listing results.

In the first part of the thesis, a state of the art will be performed. Then the computation process used in the VBA programming will be described as well as the resulting output. After that, the author will take the time to describe the finite element model used and the assumptions made for the simulation. To finish, a validation of the results obtain with the FE solid model will be made using the laboratory test. This validation will then be used to compare the obtained FEM results with the Excels one making so the V&V process. At the end of the thesis, few implementations will be proposed as a discussion.

This master thesis developed at West Pomeranian University of Technology in Szczecin - using STX Europe data - is presented in partial fulfillment of the requirements for the double degree: “Advanced Master in Naval Architecture” conferred by University of Liege and the "Master of Sciences in Applied Mechanics, specialization in Hydrodynamics, Energetics and Propulsion” conferred by Ecole Centrale de Nantes.

2. OBJECTIVES AND PROBLEM DESCRIPTION

2.1 Explanation of the Problem

Previously different calculation methods were used implemented on an Excel sheet, with or without Bending. It is relatively easy to implement a homemade code for computing the different pillars using VBA programming or any other language such as Python. But until now, this produced not really friendly user software that implies to compute the pillars one by one for each new project. Parameters such as platting also need to be defined at each time. Making an automation of this process will result in a gain of time. Recently it was decided to introduce the computation using the inertia method.

As the calculation office is using data coming from different sites and different standards, a generalization had to be made.

Then using ANSYS to check analytical results with FE model that was validated with full-scale laboratory tests will ensure to fully comply with the last regulation rules.

It is of the primary importance to notice that special care has been taken about the precise modeling of the welds in order to obtain accurate stresses in these particularly complex areas. This will be developed in the section: *3.2.2 Model.*

In order to optimize the staggering, we inputted on the Excel the loading coming from the beam hull girder global FE analysis results on particular nodes (the pillars junctions). Then analytical formulas implemented on an excel sheet were used for the optimization. The optimization process will be explained in the section: *3.1.4 Working of the program*.

As explained above, to ensure accurate results, the second phase will consist in checking the results using solid FE model and validation using laboratory tests.

As the pillar staggering calculation is directly linked to the design choices - that includes several parameters- there are no real easy to use tools available in the market for the column

calculation coupled to FEM calculation. Every company has its own way to precede using different FE software and their own-implemented codes.

Based on the theory and the given value from the classification societies, it is easy to build software calculating column buckling and pillars staggering for a given project. The difficulty comes when it has to be generalized to every project, as it will be explained later. On this thesis, buckling will not be considered.

2.2 State of the Art

In the following the author will present the methodology for calculating pillars staggering in tension and / or compression and / or bending of a longitudinal/transversal girder. This data are extracts from an intern STX document on which the author use to work during his research "*Methodologie de calcul pour les decroisements d'epontilles"*.

The calculations involve determining the scattering surfaces efforts through the weld and the surrounding structure in contact with the pillars (longitudinal and transversal stiffeners, stiffeners, deck). This will be performed at each level of the pillars and the reinforcement (see appendixes figures 1). Then for each weld throat (from standard throats used in the industry), the stress is calculated according to all possible reinforcement solutions previously defined (*see 2.2.2: Different types of pillar staggering*) and programmed in VBA. These stresses are then compared to the allowable stress using VBA routine. During the time worked at STX, the author produced more than 3000 VBA code lines.

Pillars' scantling must precede the calculation of pillars staggering on which the optimization will be made. This includes definition of the deck, flange, girder and beam thickness as well as the pillars thickness and shape (round or square) and the material.

It is important to understand well the principles of the pillar calculation and the constraints that are induced. These constraints could be mechanical or design oriented as well as financial or manufacturing linked. As an example, in the case of 4 oblique reinforcements, it will not be possible to proceed to a weld on both sides of the reinforcement. In some other case, it will not be possible to use one type of reinforcement due to space restrictions (gusset especially).

In the following section, the author will expose the different type of loading that could occur and the calculation principles used in each case. The different types of staggering will also be presented on the section *2.2.2: Different type of pillar staggering*.

2.2.1 Loading Cases

The pillar staggering are calculated on node, tension and compression as well as bending moments are taken into account at the bottom and top of each pillars. Loadings are mainly of the overall ANSYS model. Shear is neglected. Buckling is not considered.

The 5 loading combinations below can be met:

- Loading in Tension:

→ Tension (F>0) Bending momentum (Mt=0)

→ Pure Tension = T

Figure 1 : Tension

- Loading in Tension Bending:

→ Tension (F>0) Bending momentum (Mt ≠0)

→ Tension + Bending = T+F

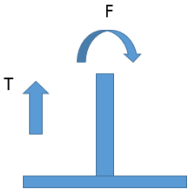

Figure 2: Tension + Flexion

- Loading in Compression:

→ Compression (F<0) Bending momentum (Mt=0)

→ Compressions pure = C

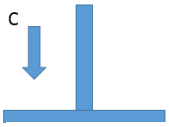

Figure 3: Compression

- Loading in Bending Compression:

→ Compression (F<0) Bending momentum (Mt ≠0)

→ Compression + Bending = C+F

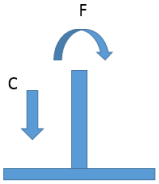

Figure 4: Compression + Flexion

-Loading in Bending:

→ Axial loading null (F=0) Bending momentum (Mt ≠0)

→ Pure Bending = F

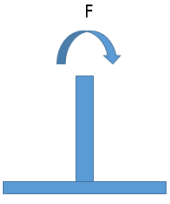

Figure 5: Flexion

2.2.2 Different Types of Pillar Staggering

Different staggering is presented below, from the lowest to the highest difficulty of implementation. The easier it is to make reinforcement, the cheaper it is, and this is also the hierarchy chosen for the optimization process:

a) No reinforcement. The beams and girders are sufficient to support the loading.

b) Gussets. Their use will depend of the available space.

c) Reinforcement oblique

d) Reinforcement uprights

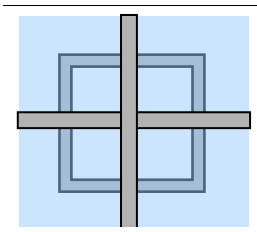

Figure 6: No reinforcement © STX France

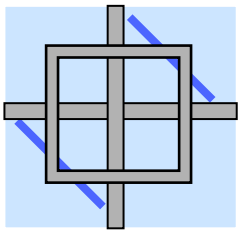

Figure 7: Two oblique reinforcements © STX France

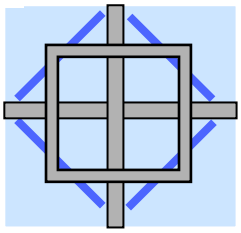

Figure 8: Four oblique reinforcements © STX France

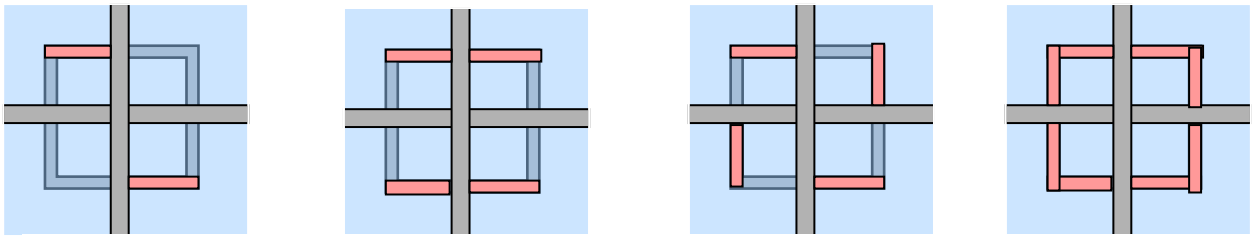

Figure 9: Upright reinforcement, 2, 4, 4 and 8 © STX France

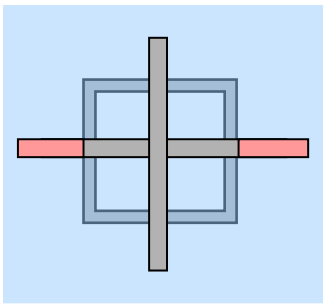

Figure 11: Two gussets on girder © STX France

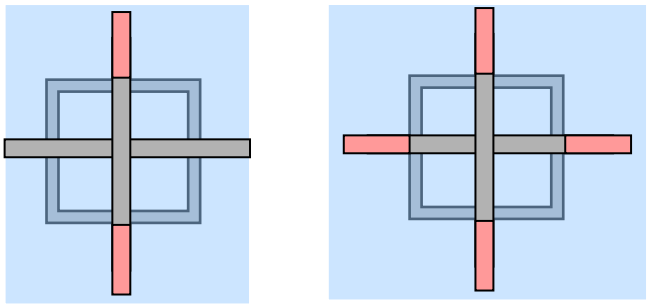

Figure 10: Two gussets on beam and four gussets © STX France

In this thesis, only the solution without reinforcement and with oblique reinforcement will be presented as the other solutions are following the same computation principle.

On the following section, the author will explain the computation hypothesis especially the one used for welds.

2.2.3 Computation Hypothesis

2.2.3.1 Relation Between Admissible Constraints and Weld

For our calculation one of the main data is the obtained stress in the reinforcement. In order to be able to compare whether the weld will be able to withstand the loading or not, we need to obtain an admissible constraint for this particular area.

It has to be noticed that welds are made in grade AH36 or equivalent quality.

The retained expression for admissible constraints, is the one given in BV 2000 such as:

- In Tension: $$\sigma_{adm} = \frac{R_{eH}}{k \times \gamma_R \times \gamma_m} = \frac{235}{k \times \gamma_R \times \gamma_m} \quad (1)$$

- In compression: $$\sigma_{adm} = R_{eH} \quad (2)$$

With:

σ_{adm}= admissible constraints

$\gamma_R = 1.2$ and $\gamma_m = 1.02$ (Reference value for the FE model for heave 10-5)

$k = 1$ for grade A, and $k = 0.72$ for grade AH36

In Tension, the weld is calculated with the equivalent constraints in the critical section. The values are computed as follow for fillet and single bevel weld:

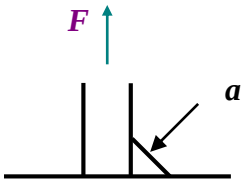

F: Effort in Tension

a: Weld depth

l: Length of welding

Figure 12: Weld model definition

© STX France

Structure in Grade A and weld in Grade AH36:

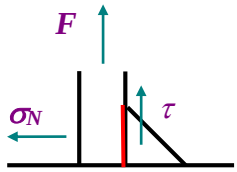

Figure 13: Structure grade A
© STX France

$$\tau = \frac{F}{al\sqrt{2}} \qquad \sigma_N = 0 \tag{3), (4)}$$

$$\sigma_{eq} = \sqrt{3\times\tau^2 + \sigma_N{}^2} = \frac{F\sqrt{3}}{al\sqrt{2}} = \tau\times\sqrt{3} \tag{5}$$

With:

$$\tau = Shear\ stress$$

$$\sigma_N = Normal\ constraint$$

$$\sigma_{eq} = equivalent\ constraint$$

Here, the weld is dimensioned in shear:

$$\tau_{adm} = \frac{1}{\sqrt{3}}\times\frac{235}{1\times1.2\times1.02} \approx 110 \text{ MPa} \tag{6}$$

$$\tau_{adm} = admissible\ shear\ stress$$

Structure in Grade A and single bevel in Grade AH36:

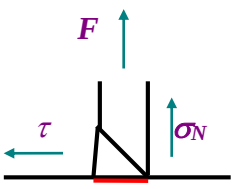

Figure 14: Structure in Grade A and single bevel
© STX France

$$\tau = 0 \tag{7}$$

$$\sigma_N = \frac{F}{1.2\times e\times l} \tag{8}$$

$$\sigma_{eq} = \sqrt{3 \times \tau^2 + \sigma_N{}^2} = \frac{F}{1.2 \times e \times l} = \sigma_N \tag{9}$$

Weld is dimensioned in normal constraint:

$$\sigma_{adm} = \frac{235}{1 \times 1.2 \times 1.02} = 192 \quad \text{MPa} \tag{10}$$

Structure in Grade AH36 and weld in Grade AH36:

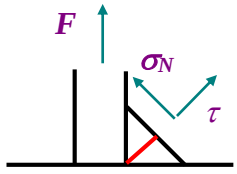

Figure 15: Structure in Grade AH36

© STX France

$$\sigma_N = \tau = \frac{F}{al\sqrt{2}} \tag{11}$$

$$\sigma_{eq} = \sqrt{3 \times \tau^2 + \sigma_N{}^2} = \frac{2F}{al\sqrt{2}} = \frac{F\sqrt{2}}{al} = 2 \times \tau \tag{12}$$

Weld is dimensioned in equivalent constraint this is “equivalent” to a limitation of shear stress to 0.5 time the admissible one:

$$\tau_{adm} = \frac{1}{2} \times \frac{235}{1 \times 1.2 \times 1.02} = 133 \quad \text{MPa} \tag{13}$$

Structure in Grade AH36 single bevel in Grade AH36:

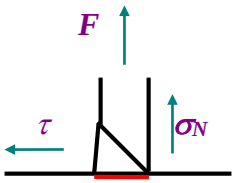

Figure 16: Structure in Grade AH36 single bevel

© STX France

$$\tau = 0 \tag{14}$$

$$\sigma_N = \frac{F}{1.2 \times e \times l} \tag{15}$$

$$\sigma_{eq} = \sqrt{3 \times \tau^2 + \sigma_N{}^2} = \frac{F}{1.2 \times e \times l} = \sigma_N \tag{16}$$

Weld is dimensioned in normal constraint:

$$\sigma_{adm} = \frac{235}{0.72 \times 1.2 \times 1.02} = 267 \quad \text{MPa} \tag{17}$$

2.2.3.2 Admissible Constraints

In this section, we will make a summary of the different admissible constraints obtain using the formulas presented in 2.2.3.1.

σ_{adm} In Tension:

Table 1: Admissible constraint in tension

		Admissible constraint (Mpa)	
		Fillet weld	Bevel weld
Structure	Grade A	110	192
	Grade AH36	133	267

σ_{adm} In Compression:

Table 2: Admissible constraint in compression

		Admissible constraint (Mpa)	
		Fillet weld	Bevel weld
Structure	Grade A	240	240
	Grade AH36	355	355

Note: This values are not to be used in slinging.

As we will see on the following section *3.1.4 Working of the program* and as said previously, these admissible constraints will be used for the optimization process to compute whether the chosen staggering type and weld size will be able to withstand the loading.

2.2.4 Welds Throats Definition

After explaining the different types of reinforcements and the admissible stresses used for the computation, the author will now describe the others parameters used in the dimensioning process. Except of the weld size, these parameters are not going to be optimized in the optimization process.

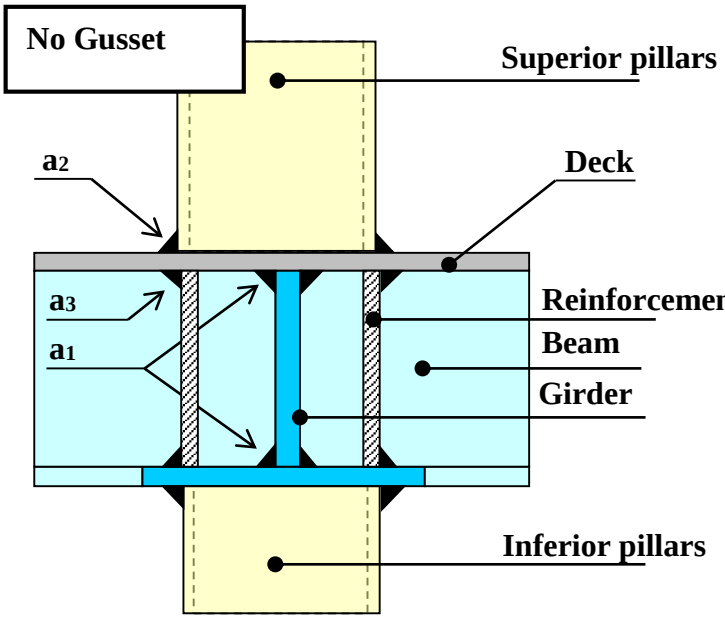

Figure 17: Staggering without gussets ©STX

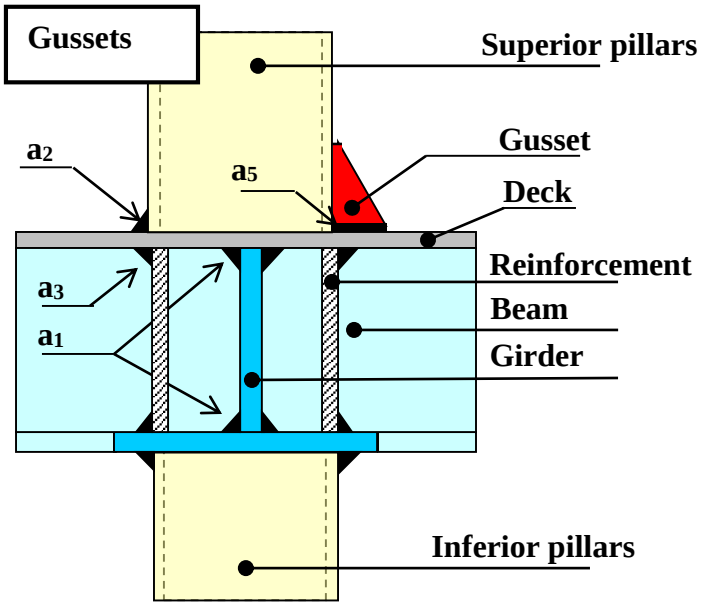

Figure 18: Staggering with gussets ©STX

Notations:

a = weld depth
pp = full penetration weld
Ep = Deck thickness
Es = Socket thickness
Eb = Beam thickness
Eh = Girder thickness
Ee = Pillars thickness
Er = Reinforcement thickness (oblique or upright)
C = External dimension of pillars (Diameter or width)
d = Length of upright reinforcement or attachment length of gussets.

It has to be noted that this thesis does not deal with vertical welds as their sizes are fixed by intern STX document *"Construction principles of pillars continuity"*.

- Throat welds (*a1, a2, a3, a5*) can take the following values: 3.5mm, 5mm, 7mm and 10mm. These are the usual weld wire used in one pass or more. In the optimization process, only 5, 8mm and single bevel will be considered.

- When reinforcements or brackets are assembled by a fillet weld, the pillars and the beams /girders are joined by a fillet weld of the same value.

- When the reinforcements are connected by a single bevel welds, the pillars are also joined together by a single bevel. The weld throat reinforcements on the web of beam / girder is a fillet weld 3.5mm value.

- In case 2 and 4 reinforcement uprights are used, they are welded by single bevel.

Table 3: Weld size available in tension and compression.

Confidential

2.2.5 Minimum Thicknesses

The minimum thicknesses of inserts, oblique or upright reinforcements and gussets are defined at bottom and top of pillars into the pillars design standard (*Intern STX document not available*). These minimum thicknesses was set using laboratory tests, workshop feedbacks and the following documents:

- *BV: Structure scantlings- Critical stress of pillar, Part 2 – Section 4-57 (January 1990)*
- *DNV: Stiffeners and pillars, Part 3 – Ch. 1 – Sec. 14*
- *LLOYD'S REGISTER: Pillars, Part 4 – Ch. 1 – Table 4 - 7*

2.2.6 Diffusion Coefficient K

The slope of a solder diffusion through the thickness of the platting is denoted by a coefficient *K*. This coefficient is used to compute the admissible constraint in the program, as we will see in the following section.

- *K* = 1, a slope of diffusion 1*E*: 1*E* corresponding to a scattering angle of 45 °

- *K* = 2, a gradient diffusion 1*E*: 2*E* corresponding to a scattering angle of 63.43 °

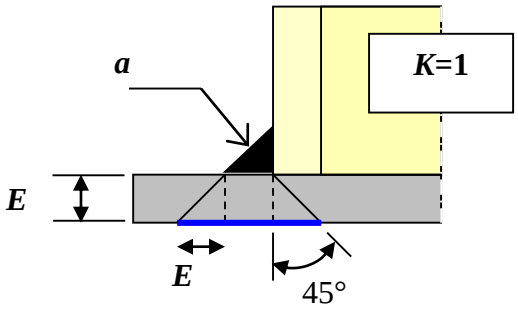

Figure 20 : Diffusion coefficient of 1
© STX France

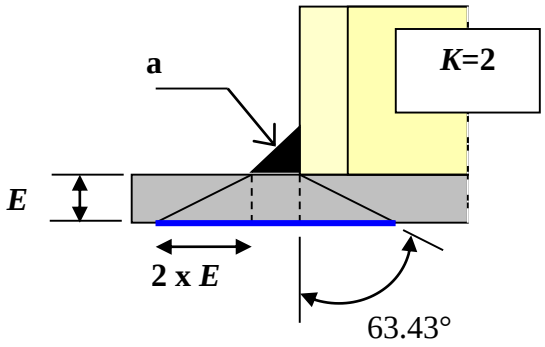

Figure 19: Diffusion coefficient of 2
© STX France

K parameter will be taken equal to 1 in order to cover the errors induced by the recovering of the diffusion areas of the welds above and under deck when it exists especially in the oblique reinforcement's configuration.

2.3 Staggering Computation in Tension

2.3.1 Methodology

In the following section we will explain the method used in the program for calculating the stress.

The permissible load in pure tension is obtained by multiplying the total area of diffusion calculated as explain on the following paragraph by the allowable tension stress:

$$T = S_{totale} \times \sigma_{adm} \tag{18}$$

The area of diffusion is the area on which we assume that the constraint will be "acting", this is the usable area for the admissible constraint. The other part of the area will not be used mainly because they are not directly welded to the above structure (important in tension) or

because they are not included in the diffusion angle and so will not have that much effect on the structure. This technique could be seen as the "collaborative platting technique" for the reinforcement.

The total area of diffusion in pure tension is equal to the minimum surface of diffusion of the addition of both the unstiffened diffusions surfaces (welding of the pillars on the deck) and the diffusion surface under bridge (welding of the beam / girder / reinforcements under the deck).

The minimum diffusion surface is equal to the surface diffusion without reinforcements plus the solution diffusion surface of the chosen reinforcement (oblique reinforcements, upright or gussets).

Note: The solutions presented below correspond to a calculation on foot of each pillar. For a calculation at pillar head, the thickness of the flange replaces the one from the deck.

As we will see later in *2.5.2 Computation principle*, these areas calculated at different level of the assembly will be used to compute the moment of inertia.

2.3.2 Solution Without Reinforcement

Confidential

2.3.3 Solution With Oblique Reinforcement

Confidential

2.4 Uncrossing Computation in Compression

2.4.1 Methodology

As some areas are considered to be ignored in the tension case, the compression and tension diffusion area are not to be the same.

The admissible load in pure compression is obtained by multiplying the total diffusion surface calculated in compression by the admissible constraint in compression:

$$C = S_{totale} \times \sigma_{adm} \tag{53}$$

The total surface of diffusion in pure compression is equal to the sum of the minimum cross section of the beam and the girder doubled for reasons of symmetry to which is added the minimum cross section of reinforcements:

$$S_{totale} = 2 \times MIN(S_b + S_{1h}) + n \times MIN(Sr) \tag{54}$$

The solutions presented below correspond to a calculation at pillar bottom. For a calculation at pillar top, the thickness of the deck must be replaced by the thickness of the flange. The footpads are no longer used.

2.4.2 Solution Without Reinforcement

Confidential

2.4.3 Solution With Oblique Reinforcement

Confidential

2.5 New Methodology

One main difference between the previous methodology and this one is that the consideration of the bending is made in stress and not in axial loading.

Converting the bending moment is achieved through the inclusion of inertia in each direction. To simplify data processing, only the sizing case will be studied. At the end only the two extremes values will be retained: one negative to be added to the compression dimensioning case, one positive to be added to the tension dimensioning case.

2.5.2 Computation Principle

We will use the moment of inertia formulation to compute the constraint that will then compare to the admissible one found in the section 2.2.3.2.

$$Sig = M / (I/v) \quad (73)$$

Sig: Constraint in MPa.

M: Bending momentum in N.m

I: Inertia of uncrossing in cm4

v: Maximal distance to the neutral axis cm.

With: $I = I0 + S * d2$ (74)

$$S = B*H \quad (75)$$

B=Beam of the diffusion area

H= High of the diffusion area

And $Io = B*H3/12$ (76)

This method is used to compute the inertia for each configuration.

Example of computation:

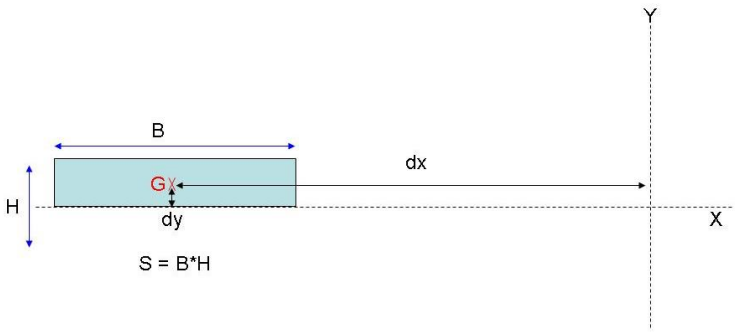

Figure 21: Momentum of inertia © STX France

$$Ix0 = B*H3 / 12 \quad (77)$$

$$Ix = Ix0 + S*dx^2 \quad (78)$$

With Ix= Moment of inertia in X

dx= Distance along X axis of the gravity center

$S=B*H$

$B=Beam$

$H=High$

$$Iy0 = B3*H / 12 \quad (79)$$

$$Iy = Iy0 + S*dy^2 \quad (80)$$

With: Iy= Moment of inertia in Y

dy= Distance along Y axis of the gravity center

Then for each weld we can calculate the total moment of inertia in both direction X and Y at the different level of the reinforcement as previously explain for the diffusion surfaces (on deck weld, on deck, under deck and on reinforcement weld).

$$Itot = \Sigma\ (I0 + S*d^2) \quad (81)$$

Then the modulus could be compute:

$$\boldsymbol{W} = Itot / \nu \quad (82)$$

In most cases, the inertia of the not reinforced configuration have to be add to the one from the reinforced configuration:

$$\boldsymbol{W} = Itot\text{-}reinforce + Itot\text{-}without\ reinforcement \quad (83)$$

In Excel macro distinction is made between the reinforcements on beam and girder in order to deal in the most accurate way with the different thicknesses between girder and beam and the particular case where there is one or the other missing.

In this thesis, only reinforcements on girder are described, a simple conversion between axis and thicknesses being sufficient to get the results of reinforcements on beam.

2.5.3 Solution Without Reinforcement

Confidential

2.5.4 Solution With Oblique Reinforcements

Confidential

3. RESULTS

3.1Tool Presentation

3.1.1 Design Choices

The software results will be directly correlated to the design choices such as reinforcement type available (*see 2.2.2 Different Types of Pillar Staggering*) and weld size implemented (*see 2.2.4 Welds Throats Definition)*. These choices are made by the design office according to the production proposals and in respect with STX intern standards (*see appendixes*). These design choices will result in input data that will be implemented in the program in different manner, as we will see in the next section. Some of these choices will be consider as parameter on the optimization process (weld size, type of reinforcement) and some other will be fixed (pillars section, position and geometry, ship scantling).

As we will develop more in the part relative to improvement proposals (*see 4 Improvement Proposals and Conclusion*), the other design choices could also later be consider as parameters.

3.1.2 Input

As explained above, one of the main input data for the program is coming directly from the hull department. It consists in results of analysis made on the global model. The geometry from amidships section and GA (*see figure 3.1.2-23*) are also important data. This data will help to define each pillar: diameter, thickness, position (GA) and forces (ANSYS). The amidships section will help to define the deck, girders and beam size, material data and positions. This ANSYS input will consists in as many lines as there are nodes for each pillar in the global model. Generally speaking, each pillar is modeled by two nodes.

Confidential

Figure 22: ANSYS data on node: node position, top element number and geometry, bottom element number and geometry

Confidential

Figure 23: Amidships section data.

All this data has to be changed for each project and are not considered as optimization parameters in the optimization process but only as “model” parameters.

In addition of this data, the different reinforcement types and weld size on which the optimization process will be done are implemented directly on the code. This data will be considered as optimization parameters and are assumed to be fixed (among a certain range) for every project (*see 2.2.4 Welds Throats Definition).*

3.1.3 Output

Two different output presentations are available depending that the user is running the manual or the automatic program. On the manual one, the output will be a summary of the results for the studied pillar as display on table 3.1.3-4. It then possible to modify the pillar geometry (Beam and girder thickness, pillars diameter...) and to run again the program to see the effect of the manual geometry modification on the reinforcement and the weld size that are automatically choose.

Table 4: Example of results for the manual process. (Manual process)
Confidential

In table 3.1.3-4, the optimum weld will be a single bevel with four oblique reinforcements.

The second output type is a listing produce for the design office. It consists in the pillars positioning and definition as well as the optimum weld size and staggering type.

Table 5 Listing of the staggering type and weld size. (Automatic process)
Confidential

In this type of output, no modification of the geometry is available. If the designer wants to modify one of the pillars - because the proposed staggering type or weld size is not suitable (for space problem for example) - then the manual program should be used. These data are then introduced in the global model and in detail drawing for the production department.

3.1.4 Working of the Program

On the following diagram (larger version available in the appendixes) the different procedures used in the calculation process are displayed. As more than 3000 code lines were written, displaying them would not be possible.

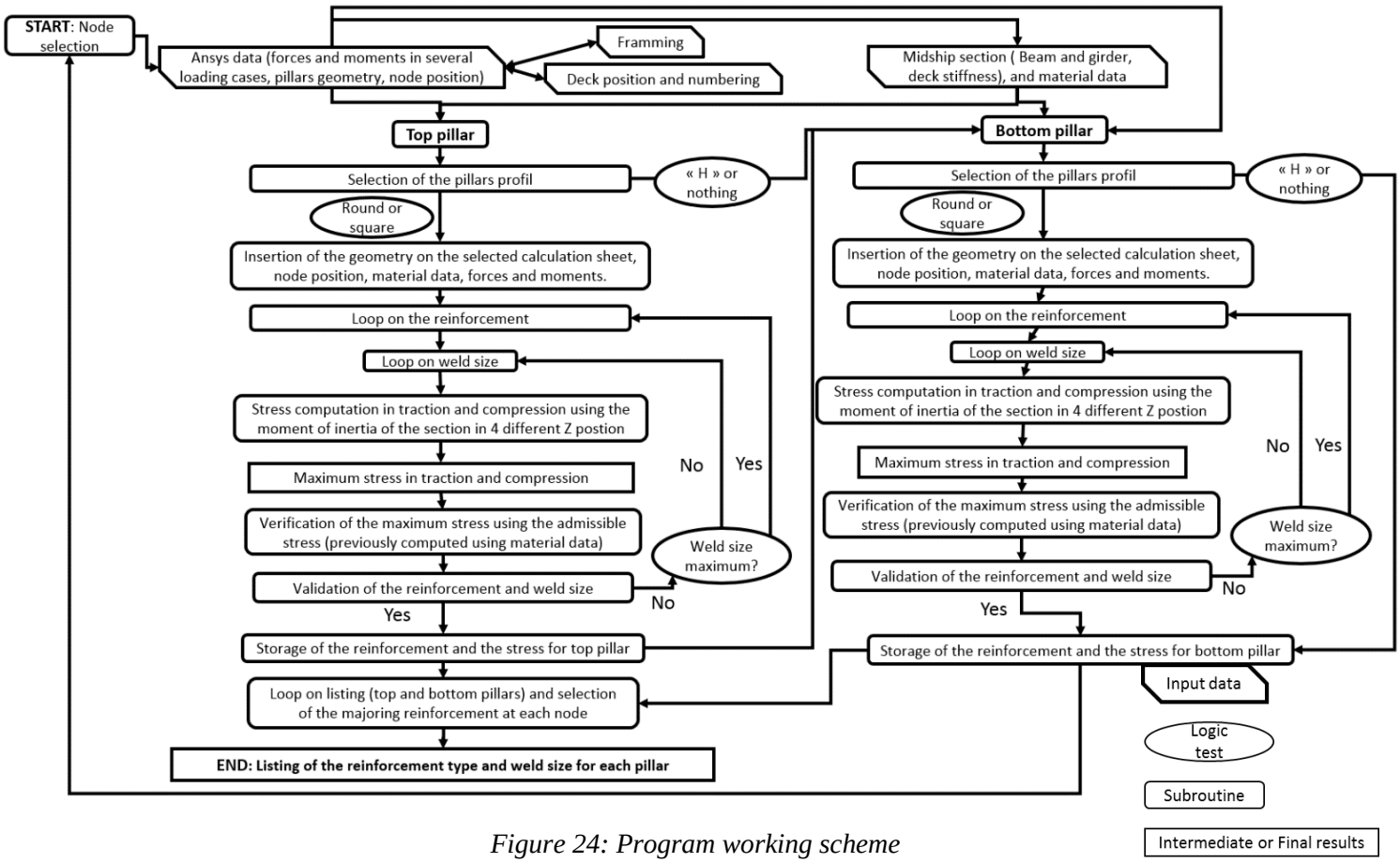

Figure 24: Program working scheme

The first step of the process manual or automatic is to input the different data such as amidships section for the decks, beam and girder dimensions. Framing, deck position and numbering are needed in order to be able to localize any pillars of the project (pillars are located by frame/deck/transversal position). Material data are also part of the inputs (maximum admissible stress). In addition, the ANSYS data coming from the global model should also be inputted. They consist in reaction forces and moment applies in each pillar in different loading cases (hogging and sagging), but also nodes positions and pillars geometry. At this stage, the reader should remind that this step was already briefly explained in the previous section 3.1.1 and 3.1.2.

Then in a second step, if the process is manual, the user have to select the position of the pillars that he is wishing to compute using the frame/deck/transversal position filter. In the automatic process the user simply select the first proposed pillar in the list. And then press the "calcul décroisement ronde ou carrée"button. When using the program in full manual mode, the previous step of input data could be deleted as the user could do it directly through the interface.

Confidential

Figure 25: Selection of the position in manual mode and launching of the process

When the pillars are selected and the button push, the program will copy the data from the ANSYS global model into the excel macro one by one in order to proceed to the calculation of the maximum stress using the moment of inertia formulation as explain on the section 2.5. This maximum constraint could be obtained in compression, tension or by a combination of the momentum and tension or compression as we are studying the envelope case (*see 2.5 Methodology*).

After selecting the type of profile (round or square) according to the imported ANSYS data, a first loop is made on the staggering. The program will try first the solution without reinforcement with the smaller available weld size. Then at the end of this process, a verification of the maximum constraint is made and compared to the admissible one. If the obtained constraint in any of the study loading cases is bigger than the admissible one, the program will first try to increase the weld size before going to a more complex staggering type (*see hierarchy in 2.2.4 : Welds Throats Definition*) .

At each loop a test is performed on the constraint, if the calculated constraint is less than the admissible one, then the weld size is validate and the program move to the next pillar.

It has to be reminded to the reader that the type of reinforcement include in the loop and the weld size are defined in the code as explained on section *3.1.2*. These are not supposed to be modified as the different possibilities were established with the different services in accordance with STX standards. The author would like to remind that the loop is assuming a

constant thickness of the reinforcement plates as the reinforcement plates are not considered as parameters (neither is the pillar). This will be discussed in the section *Improvement proposal and Conclusion.*

At the end a listing is produced (*see table 5*) proposing for each couple of pillars (top and bottom one) a suitable staggering type and weld size. In the case where a top pillars will need a stronger reinforcement type than the bottom one or the opposite, the selected reinforcement and weld size will be the strongest one.

In the listing, a reminder is made about the pillar geometry (profile and dimensions) as well as the position. This allows the designer to check the results and so avoid any possible mistake on the production drawings.

With the manual process, the results produced (see table 4: Example of results for the manual process) also display the resulting constraints in traction and compression (*majoring case as seen in 2.5 Methodology).*

3.2FEM Analysis

3.2.1 V&V Process

In order to verify and validate the results obtained using the excel program, a FE model was made. This model will be used to check the listing data in order to avoid costly over quality. Indeed, the FE model is supposed to be more precise than the analytical one (especially due to the safety coefficient and diffusion areas used on the computation for the admissible constraint (*see 2.2.3.2 Admissible Constraints)*. This 3D solid model will be validated comparing the results with some laboratory experiments.

On the above figure the general Verification and Validation procedure use in the engineering process is display.

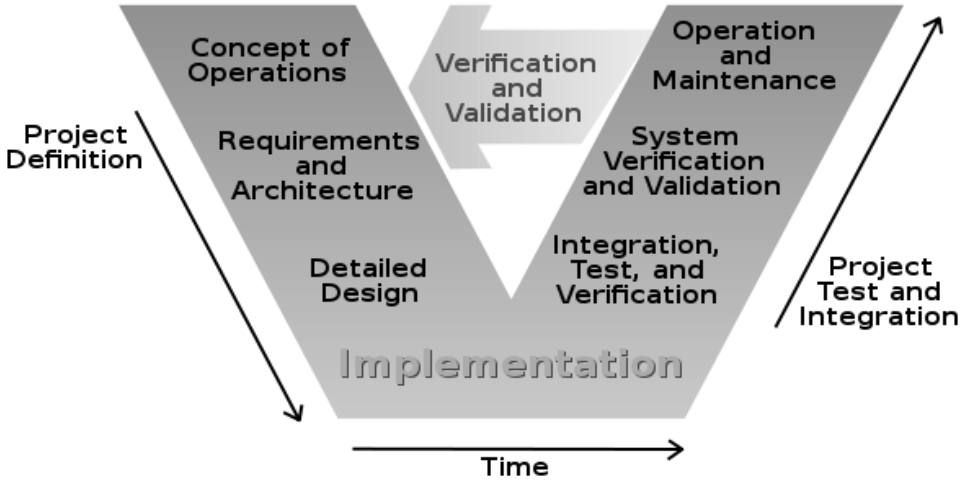

Figure 26: The V&V process

In this case, the requirement and architecture of the software was designed according to intern standards and meeting with the different involve department (Hull department, design office and production). The detailed design consists in the excel macro; its testing and integration component will be performed using the FE model and the laboratory tests. The maintenance process of the program will then be made using the same FE model (if a type of reinforcement is add for example or if a weld size is add).
This process ensures to fully comply with the ISO 9001 Quality management systems[1].

3.2.2 Model

Two different procedures were used to perform the model. The first was to use ANSYS programming language APDL to produce geometry and a meshing. Defining the parameters on the top of the script will allow to consider them as global parameters. As it will be explain in the next section, this procedure faced few design problems. In a second time, the use of ANSYS workbench allowed to perform easily a parametric geometry and analysis.

To be able to validate the model, it was decided to use the same geometry than the one tested in laboratory. As it will be explained more in detail in the following section, the model is a parametric one, so it will not be difficult to modify the model for any geometry in the future. This will then make the validation of any pillar reinforcement possible. In both models,

[1] ISO 9001 Quality management systems : refer clauses: 7.3.5 Design and development verification and 7.3.6 Design and development validation)

APDL and ANSYS workbench, the choice was made to use solid element in order to improve the precision of the results.

3.2.2.1 APDL

As explained above, the first trial for the parametric design of the pillars was made using APDL programming. This part happened to be very long and laborious especially regarding the meshing. More than 1300 code lines were produced (*see A5 APDL Code).* As the geometry includes several small details, it was important to smartly divide the geometry into mappable volumes. These small details - mainly occurring because of welds - could not be deleted, as they are the areas of interest. These details are the reason why a 3D solid refine analysis was performed. Otherwise, the author could have use the preprogrammed ANSYS option for modeling welding assembly. But as the aim was to have a precise understanding of the constraints in these particular areas, simplifying the model will not have been convenient.

To briefly explain the procedure, the macro use the following usually used steps:

1. Parameters definitions
2. Geometry definition from bottom to top
3. Weld definition
4. Cutting of the different volume for the meshing
5. Cleaning of the model
6. Boundary condition definition
7. Loading definition
8. Element definition
9. Meshing
10. Solution

The APDL macro is produced in appendixes but as this solution was not retained - due mainly to meshing problem - the author will not write much more about it.

3.2.2.2 Workbench

For the FE model, it was decided to use only a half model cut on the XY plan. This choice was made after results comparison between the full model and the symmetric one, as we will see in the following section. This allows -by saving CPU time- to perform more analysis using a more refine mesh in less time. An extra symmetry could also be apply on the ZX plan but will require more complex boundary condition in the reinforced case. However, a double

symmetry model was produced for the case without any reinforcement. Until now, the symmetric model for 2 oblique does not produced satisfying results.

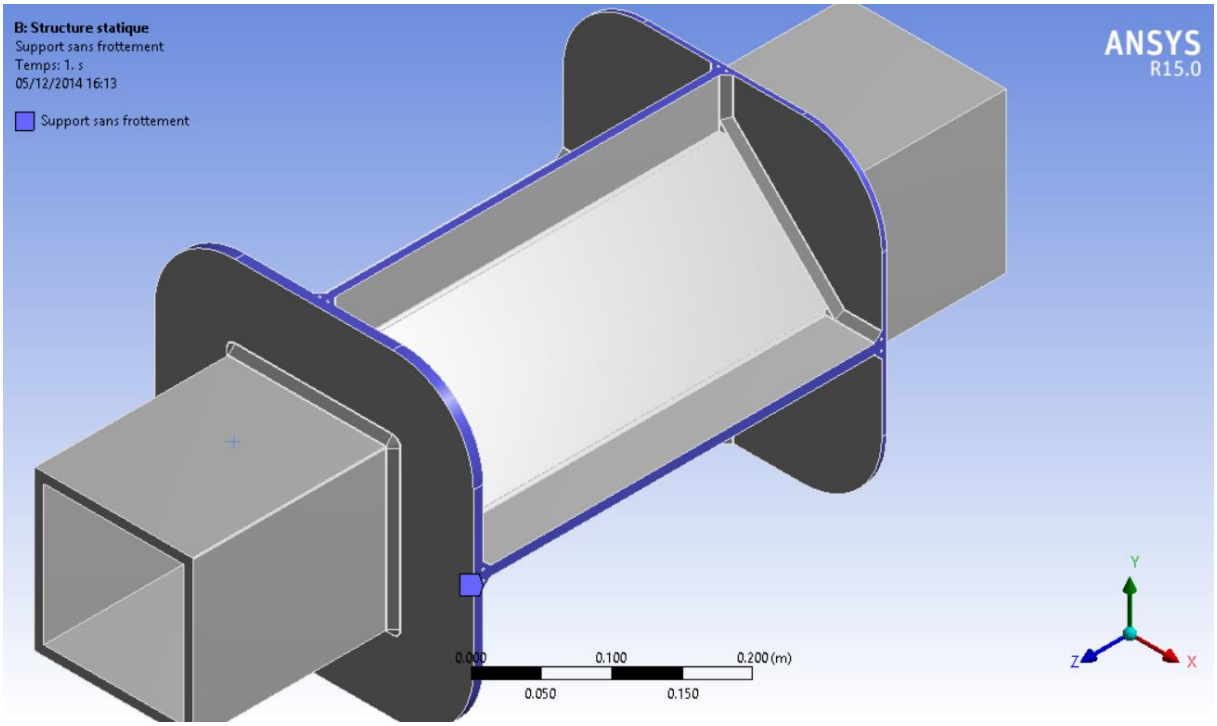

Figure 27: 2 oblique reinforcements square Workbench model without symmetry

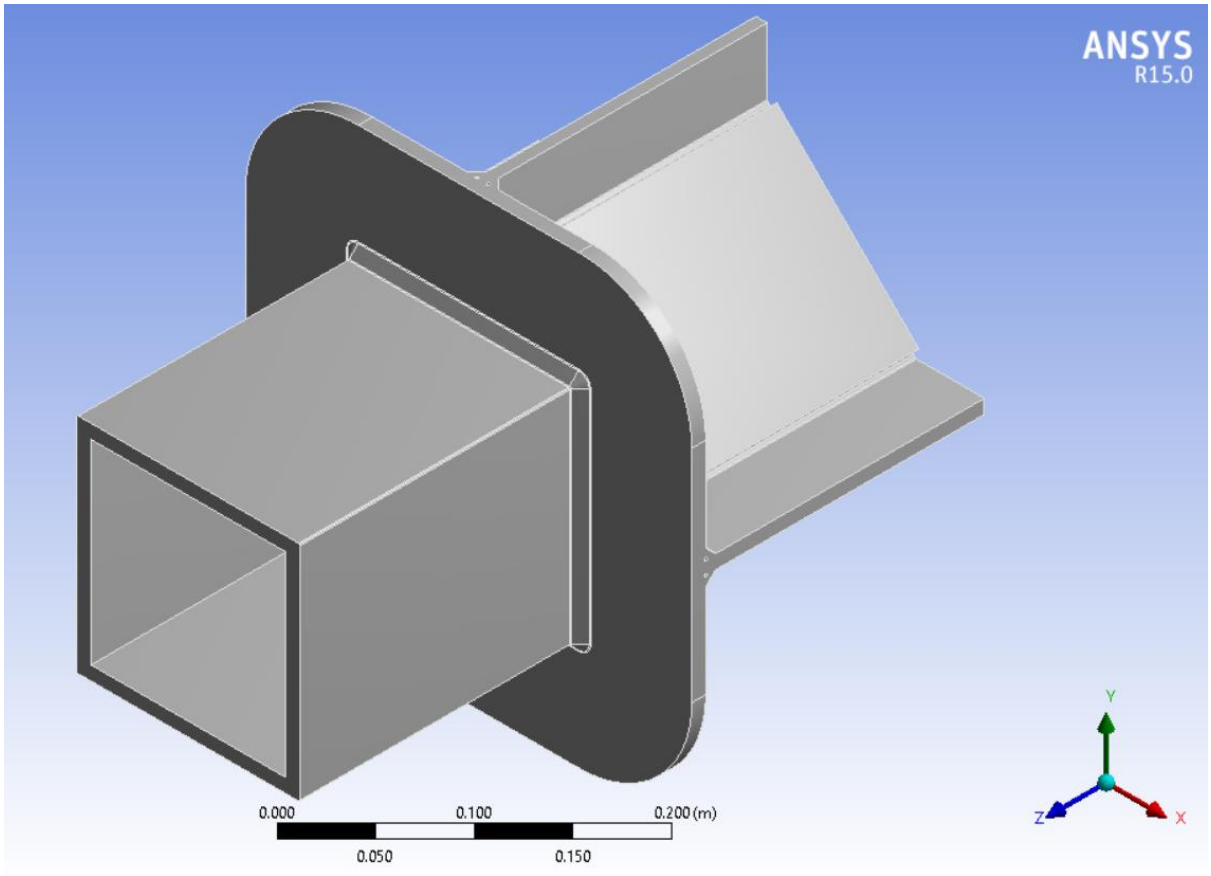

Figure 28: 2 oblique reinforcements square Workbench model with XY plan symmetry

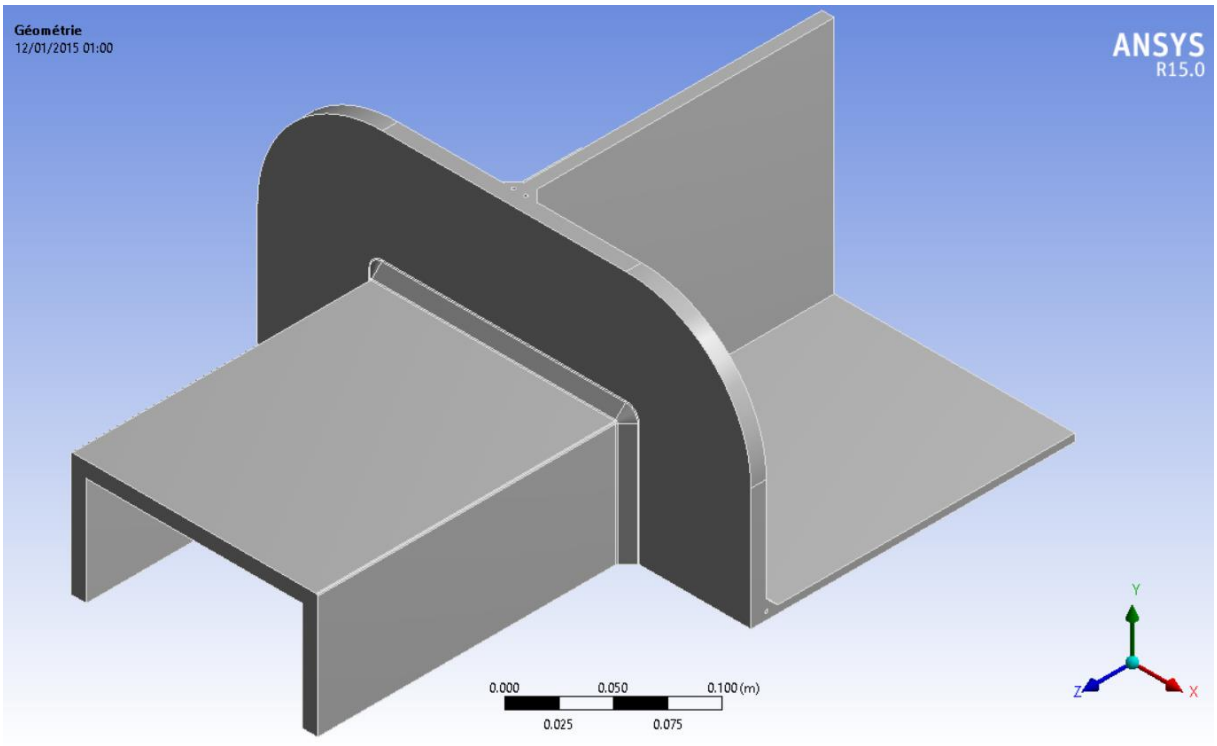

Figure 29: No reinforcement square Workbench model with XY and XZ plan symmetry

For the modeling, the author followed a 3D model using 3 circles of x mm radius situated at the root and top of the weld in order to represent the various welding defects. This model configuration does not take into consideration the welding deformations and residual constraints resulting from the welding process. This model was based on previous research made on welding modeling. Unfortunately the author is not able to display the article here.

In the following diagram, we can observe the pillar (vertical yellow rectangle) separated from the deck (horizontal yellow rectangle) by a x mm space resulting from the designed weld. As we will explain later, this area will be consider to be in contact in the Z direction with the deck (distant contact condition). It is also possible to observe a big quarter of circle in yellow; this circle is used as a parameter for the weld throat size. All the different welds were model using this scheme and then extruded.

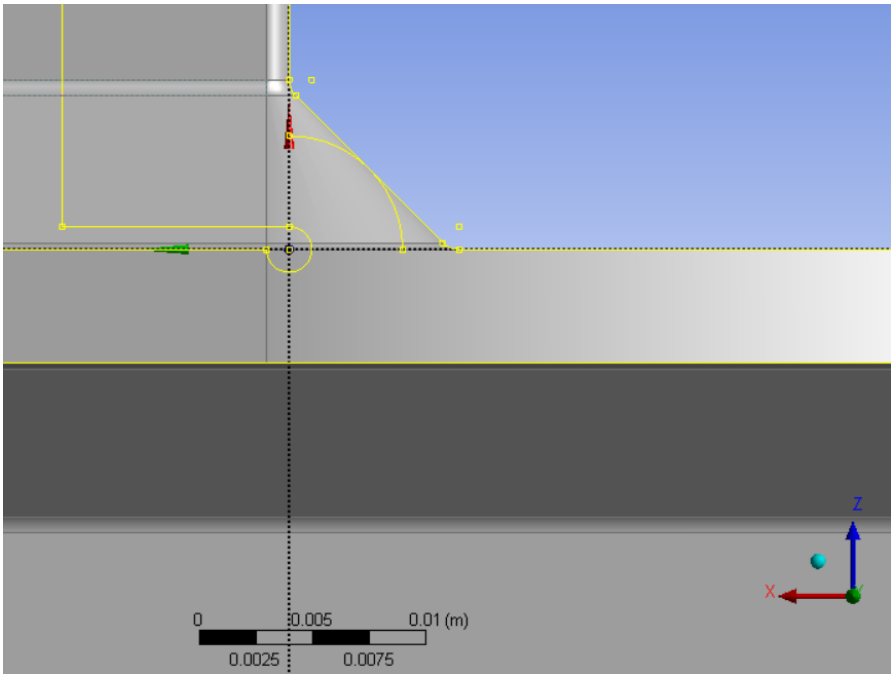

Figure 30: Weld between the pillar and deck Design Modeler sketch

In the previous figure (3.2.3-30) we can observe that only the fillet weld was taken into consideration. As the single bevel welds will be treated as a fully continuous material, it does not require any special model.

Using this sketch in workbench allows to easily define a model for the round profile pillar that is display in the following diagram. At this stage, as no laboratory tests were performed on

round pillars, no comparison of the results obtained using the FE model was made. This will be done in a close future.

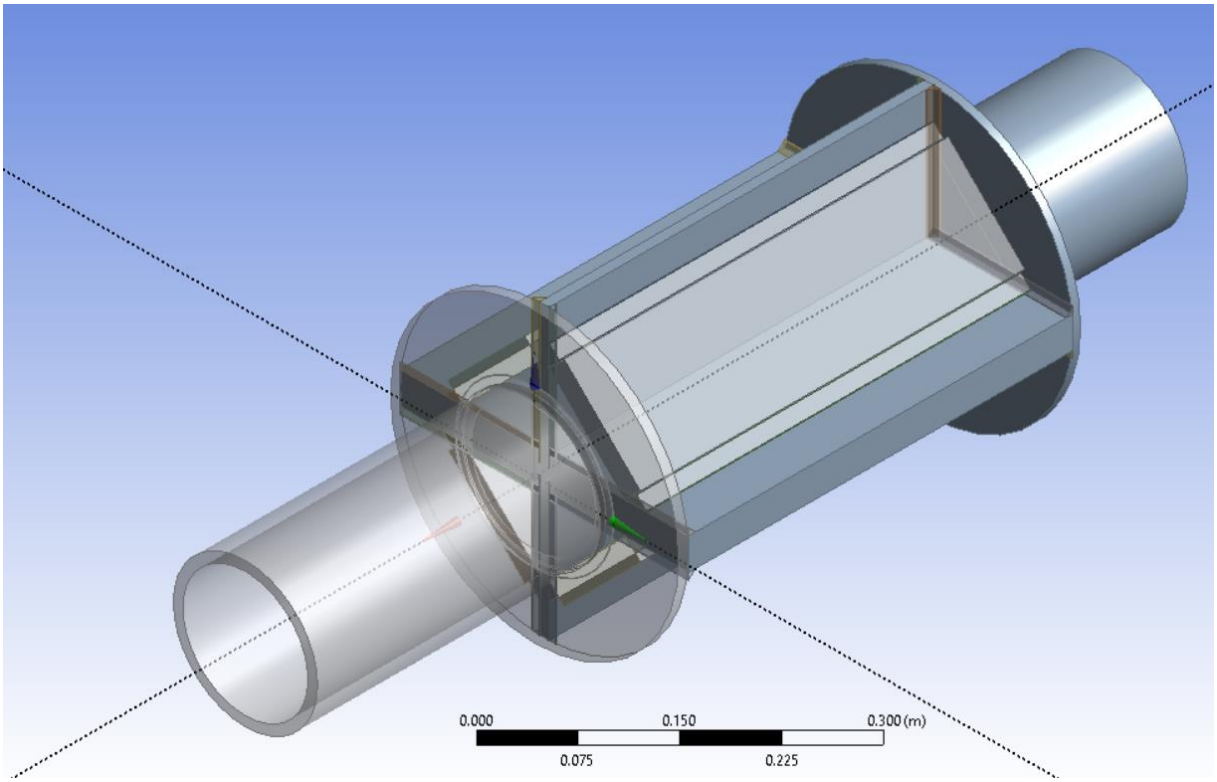

Figure 31: ANSYS workbench parametric model for round pillar

3.2.3 Parameters

In order to be able to compare our results with the experimental ones, the author choose a set of parameters as the ones used during the laboratory experiments (*see 3.4.3: Comparison with laboratory test).*

As explained previously, the main fixed parameters are the one provides by the GA and the amidships section. This includes beam and girder, deck, flange and pillar thickness as well as pillar diameter. In addition, weld throat and number of reinforcement are provided as optimization parameter.

Table 6: Table of parameter used for the square model (in French)
Confidential

On the table 3.2.4-6 the reader can observe that some of the parameters are not consider in the optimization process such as the angle of the oblique reinforcement and the angle of welds (only fillet welds are consider).

The author would also like to remind that the model was made in accordance with STX intern design standard and so reinforcement platting size is directly correlated to the pillar diameter. For round pillars, the oblique plate length will be equal to 0.75*pillar diameter and for square the plate will be equal to 0.9*pillar's beam (*named as C in the previous table*).

3.2.4 Boundary Conditions

For the boundary condition of the model, the author use to set the girder and beam as simply supported as well as the deck and flange. The author also chose to have the inferior pillar set as fixed.

These choices were made in accordance with the laboratory test conditions as we will see in the comparison section.
These boundary conditions are also the one matching the more the real working conditions of the assembly.

The following figure display in blue the boundary conditions.

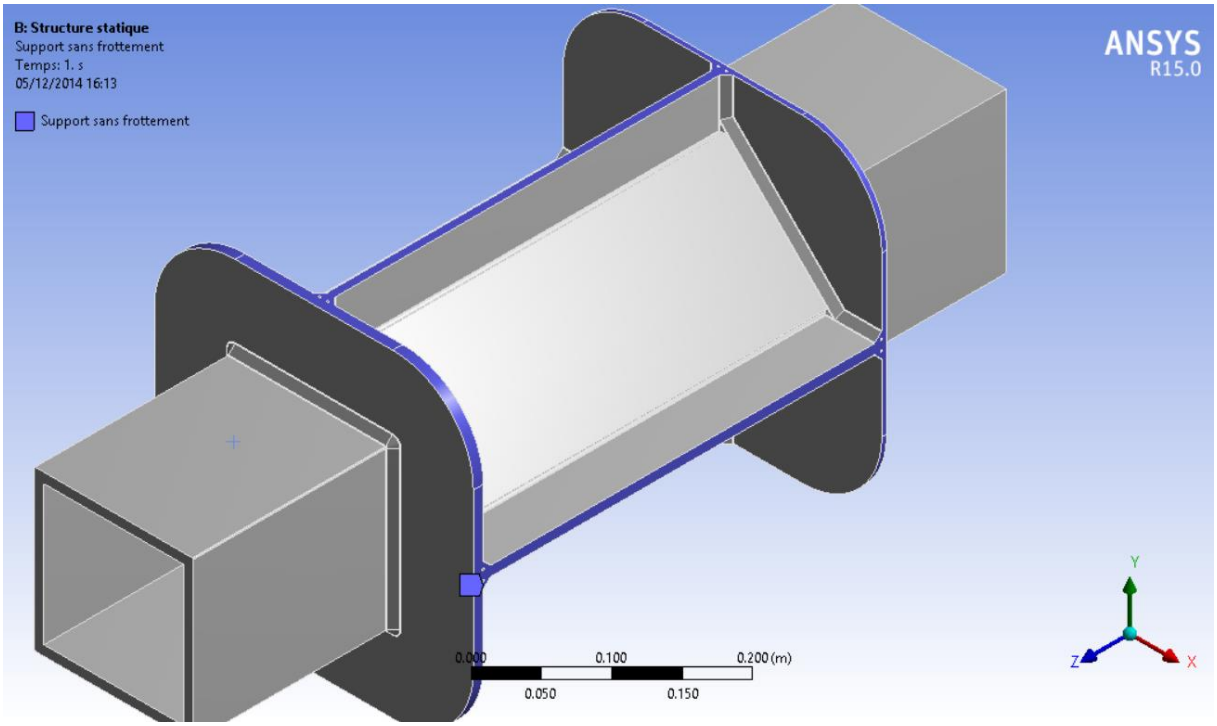

Figure 32: Deck, girder and beam as well as flange set to simply supported

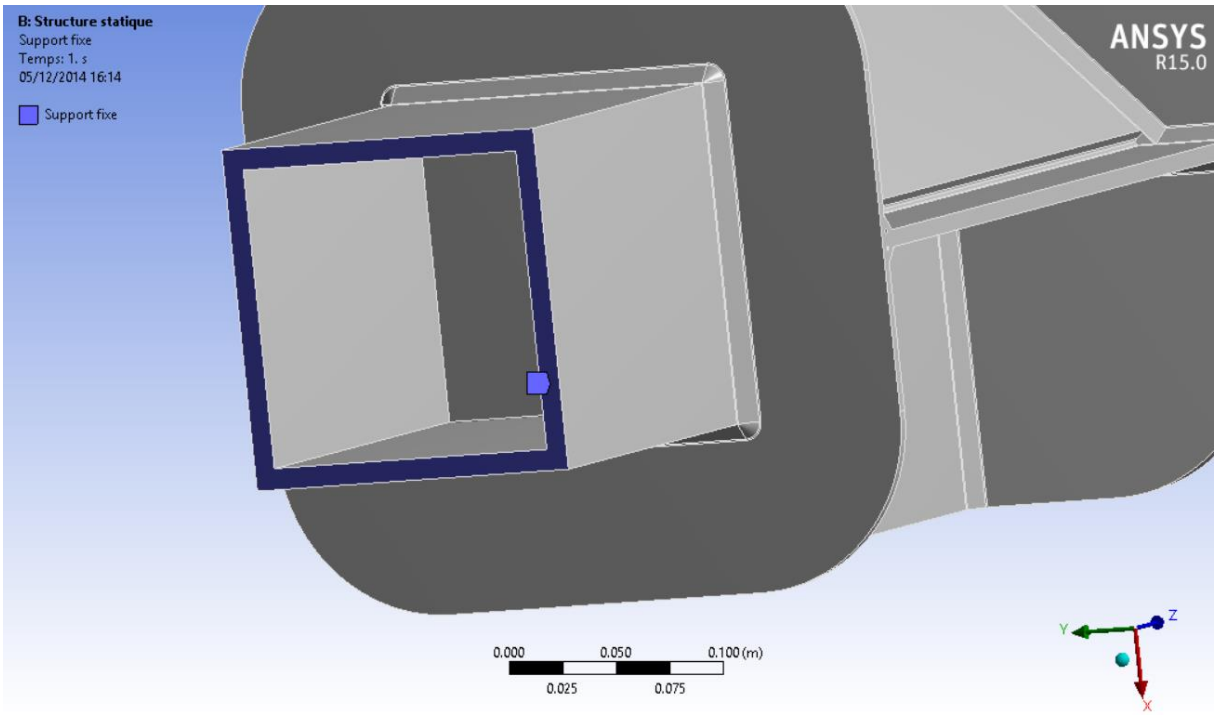

Figure 33: Bottom pillar cross-section set to be fixe

It was also important to well define the contact areas especially at the pillar and deck junction, as well as the pillars and flange junction. This contact will be acting only in compression cases in order to match as closely as possible the reality. Indeed, this part of the pillar is

usually not perfectly connected to the deck when fillet welds are used. As both contact areas are not in contact in the model due to the defects modeling (see figure 3.2.2.2-26), we had to set distant contact. The initial contact distance is fixed to x mm witch is the equivalent of the defect radius.

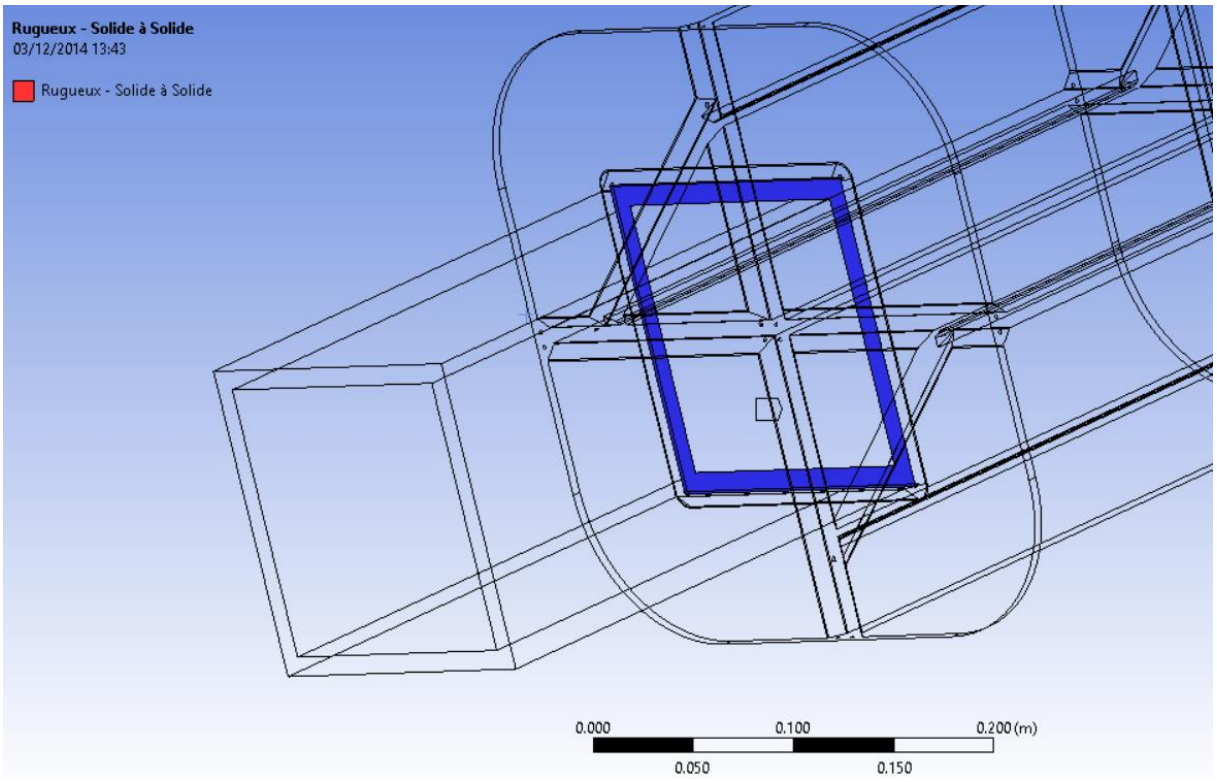

Figure 34: Contact area on the bottom of the top pillar (square model without symmetry)

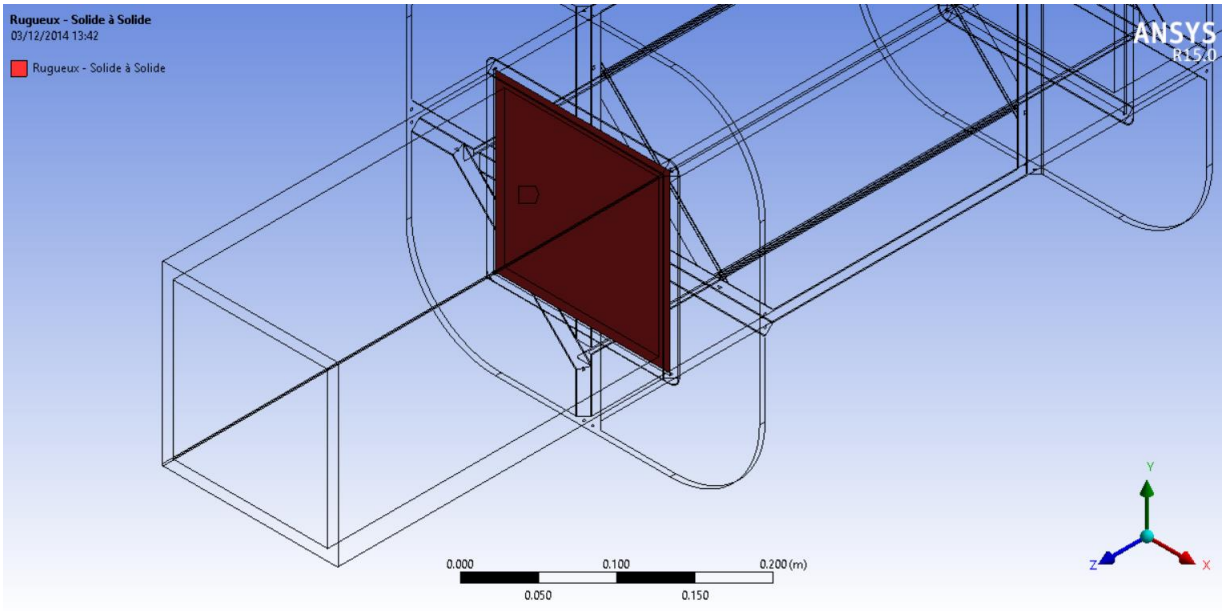

Figure 35: Contact area on deck (square model without symmetry)

In the case of the symmetric model, we simply add a symmetry area on the ZY plan. For the fixed condition on the bottom pillar, it was only moved along the Z-axis as it appears that the main constraints are on the weld between pillar and deck and not in the reinforced area. No symmetry condition was used in that case (no symmetry condition in the XY plan).

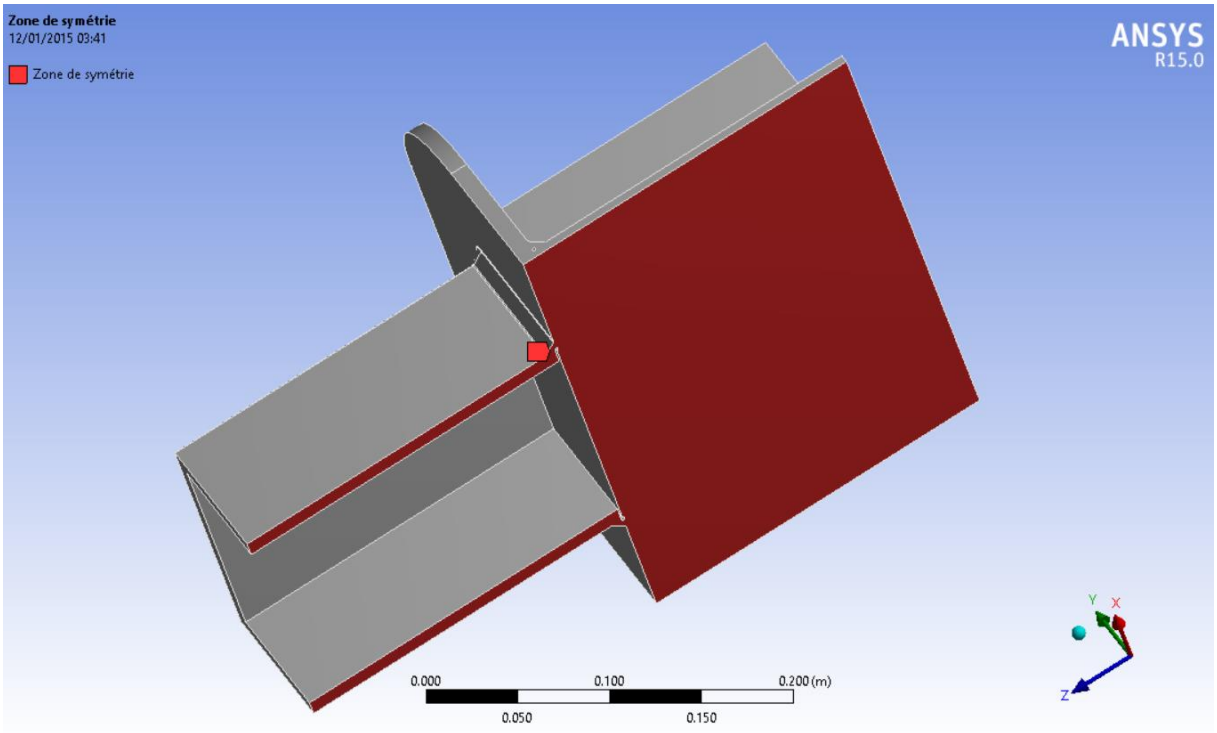

Figure 36: ZY symmetry condition

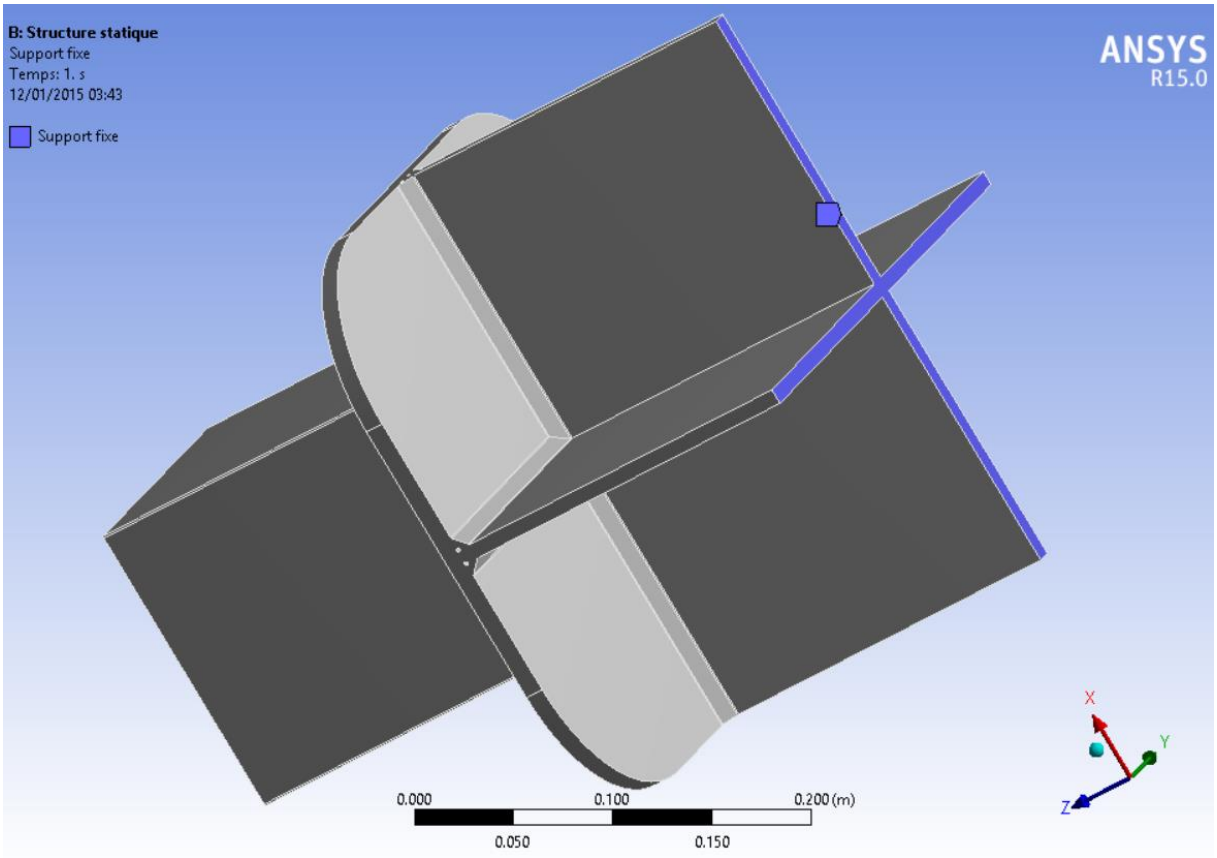

Figure 37: Fixed boundary condition on the plan of symmetry XY

3.2.5 Loading

For the laboratory test, a tension force was applied on one lateral face of the pillars at 0.96 meter from the deck (or the flange depending the case). As the modeling of 0.96 meters of pillar will appears to be time consuming in the calculation process and that the displacement measurement was taken at 0.2 meters from the deck, the author choose a pillars height of 0.2 meters and then apply proportional momentum and forces.

The author simply used the following formulas:

With an arm lever of 0.96 meters for the laboratory test:

$$\sum Fr = 50000 \text{ N} \tag{84}$$

$$\sum Mr = 50000 * 0.96 = 48000 \text{ N.M} \tag{85}$$

With $F_r = Apply\ force$

$M_r = Resulting\ apply\ moment\ for\ model\ test$

Using an arm lever of 0.2 meters for our FE model:

$$\sum Fe = 50000\ \text{N} \tag{86}$$

$$\sum Me = 50000 * 0.2 = 10000\ \text{N.M} \tag{87}$$

With $F_e = Apply\ force$

$M_e = Resulting\ Apply\ moment\ for\ the\ fem\ model$

It is then easy to observe that

$$\sum Mr - \sum Me = 38000\ \text{N.M} \tag{88}$$

So in addition of the 50kN force a momentum of 38000 N.M is apply to obtain equivalent conditions.

For all the different loading cases studied -going from 20 KN to 120 KN- the same procedure was used.

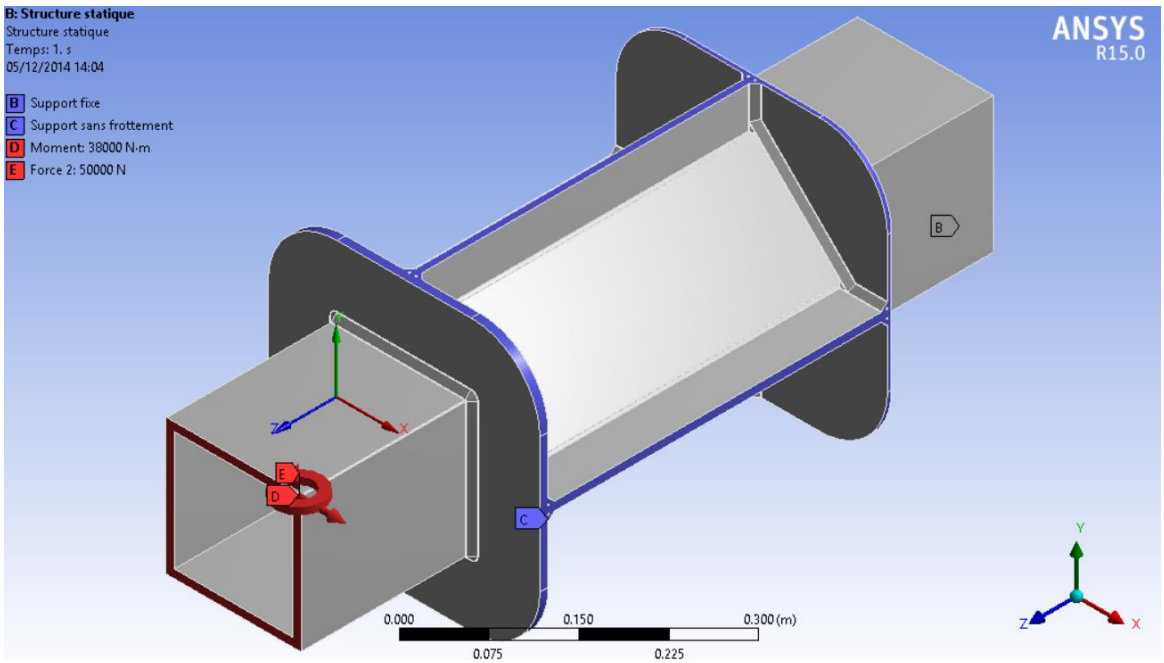

Figure 38: Moment and forces apply on the FE model at 0.2m from deck

In the above figure 3.2.5-38, the moment and axial force are displayed on a full 2 oblique model.

In case of a symmetric model, the forces are reduce in consequence without forgetting to apply the symmetry condition.

When applying a load on a surface with ANSYS, except if the load has been defined to be a pressure, the load will be apply at the center of gravity of the selected area using a distant point.

3.2.6 Material Data

For the FE model, structural steel having Young modulus of 2 E11 Pa, elasticity limit in traction and compression of 2.5 E8 Pa and a maximum tensile stress of 4.6 E8 Pa was used. These values were chosen in accordance with the steel used during the laboratory tests (see 3.4.3: *Comparison with laboratory tests*).

3.2.7 Meshing and Mesh Convergence

In order to give an idea of the time needed to run the simulation, the author would like to inform that the analysis were performed on an Intel Core i7 3517U with 4GB RAM (Extra virtual memory available up to 100GB).

Several meshes were studied. At first the global model was mesh without the help of any symmetry. The resulting data are displayed on the following diagram.

```
***** ROUTINE COMPLETED *****  CP =         8.766


--- Number of total nodes = 775778
--- Number of contact elements = 2080
--- Number of spring elements = 24
--- Number of bearing elements = 0
--- Number of solid elements = 509700
--- Number of total elements = 511805
```

Figure 39: Mesh statistics

As it can be observe on the figure 3.2.7-39, using linear solid tetra element, the number of elements obtained is around 500K. Spring elements were used in order to avoid rigid body motion.

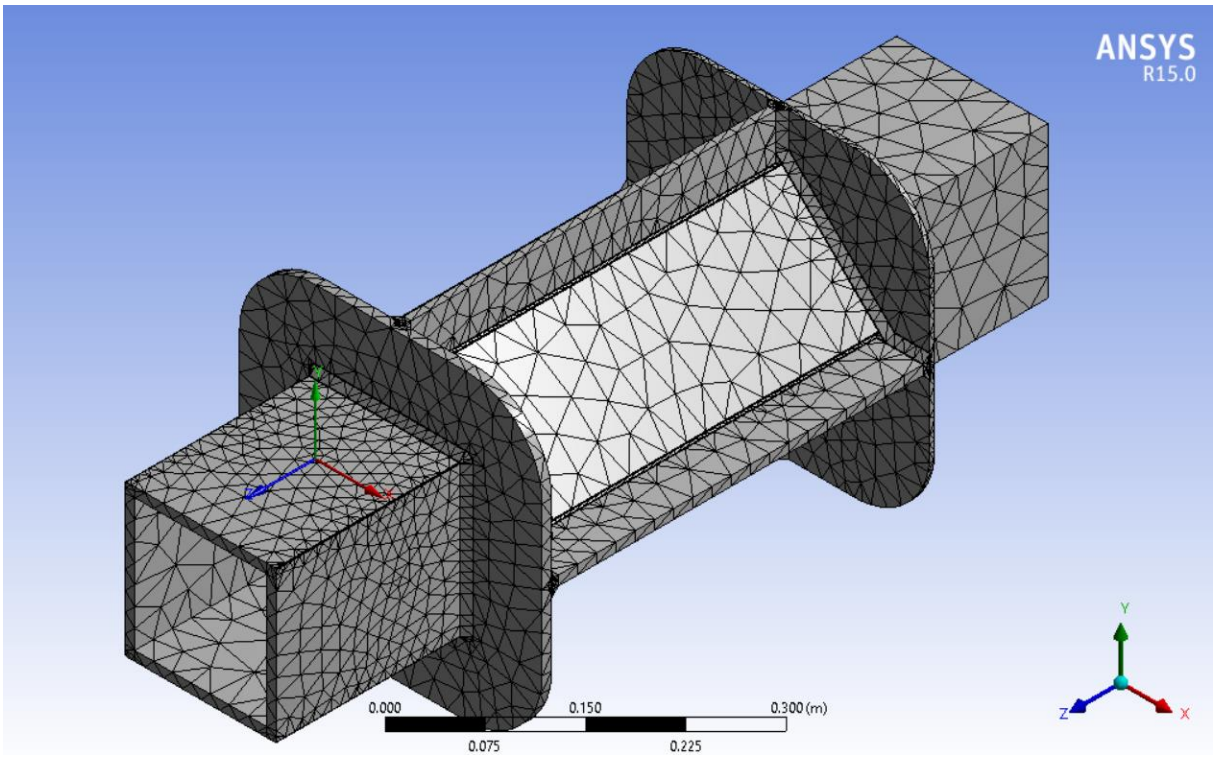

Figure 40: Coarse mesh on the global model

To study the mesh convergence, the first step was to perform a visual check locally and globally of elements shape. Then setting the ANSYS parameters to a growing ratio of 1.2 with fast transition, minimum element length of 7.854e-004 m and transition ratio of 0.272 allowing to obtain an accurate mesh.

In order to be able to compare our different mesh, the study of convergence was made on the displacement.

For the model display in the figure 3.2.7-40 a displacement of 1.8527 mm was measured when applying a force of 70KN. These results were obtained using linear behavior elements. This was one of the first analysis run.

In order to model the welding defect, three one mm diameter discs were used. On the figure 3.2.7-40, it is possible to observe this defect for the two-welded junction of the girder/beam

and the deck/flange. At this particular points, it can be observe that the mesh is extremely refine whereas it is rather coarse in the other areas. Observation could be made of all connections between weld and parts that are correctly performed in the mesh.

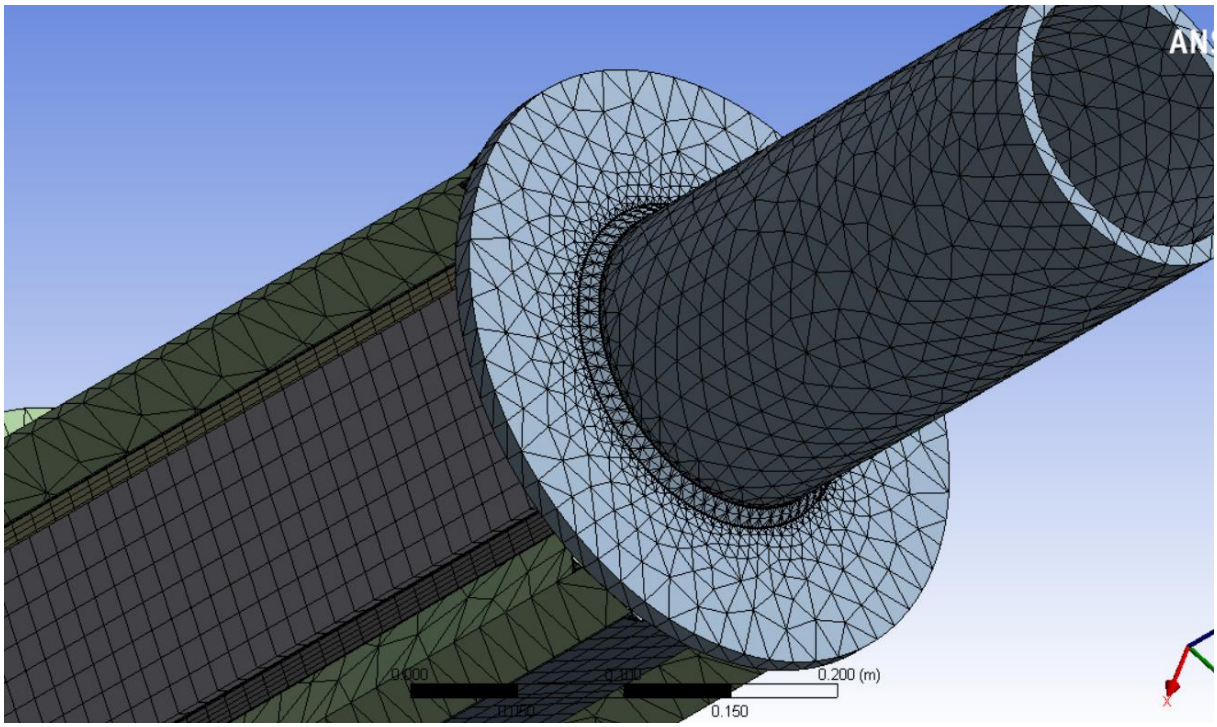

Figure 41: Global mesh for round model

On figure 3.2.7-41, a very good mixed mesh is performed but unfortunately the meshes connections between welds and parts are not correctly achieved. This will be solved in the future with a deeper study of the round model.

For the entire following model, we activate the mesh morphing. Activating morphing helped to automatically refine the mesh in the detailed areas, additionally with the other sizing parameters.

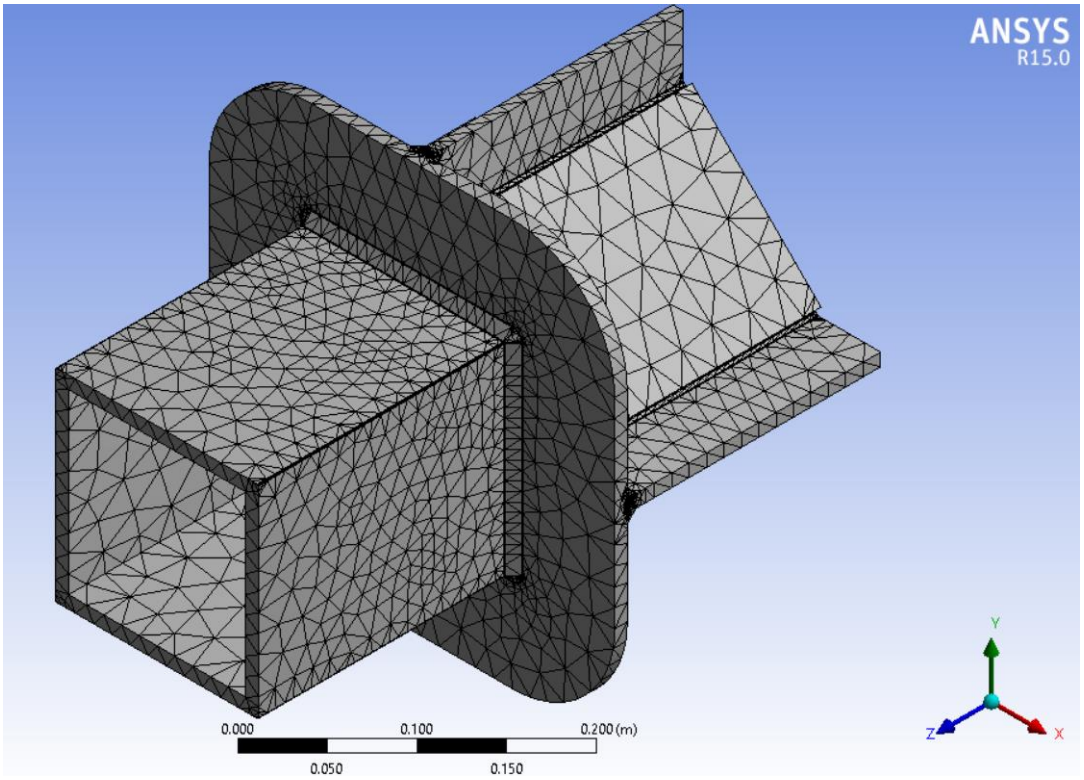

Figure 42: Coarse mesh model with 2 oblique reinforcements – 227614 Elements, 354990 Nodes

For the model display in the figure 3.2.7-42 a displacement of 1.7138 mm was measured when applying a force of 70KN. This result was obtained using coarse mesh having 227614 elements. For that configuration the simulation was run in a few minutes.

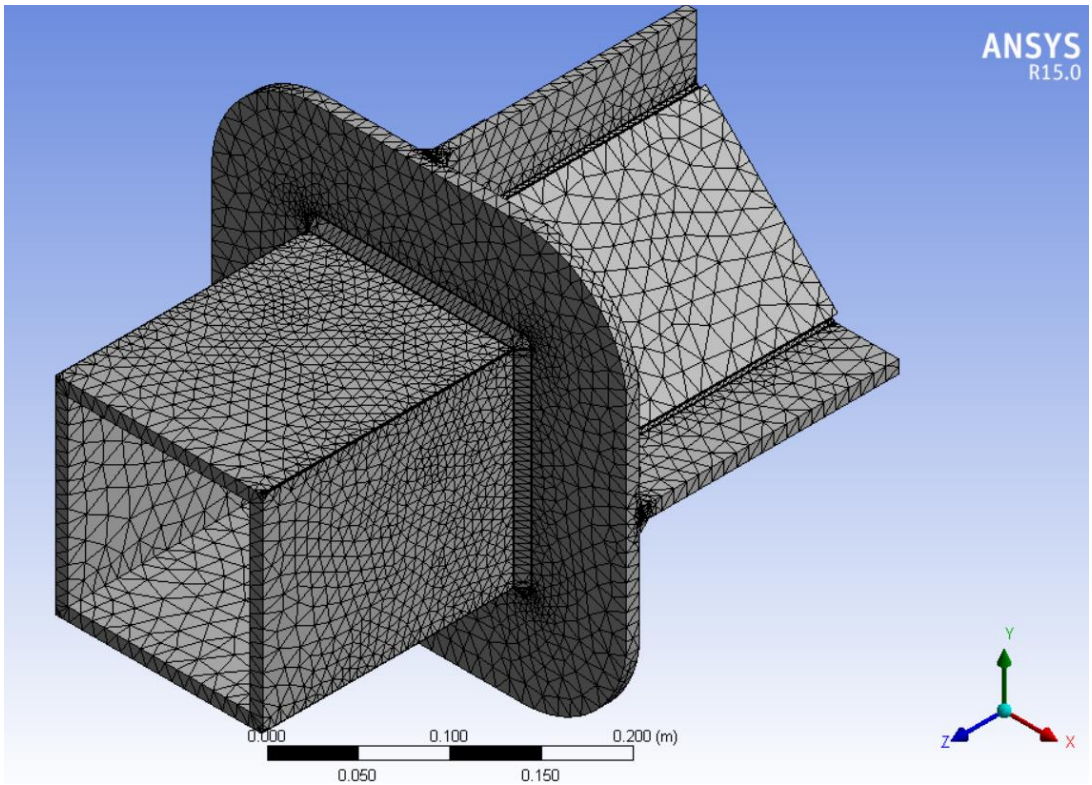

Figure 43: Fine mesh model- 904040 Elements, 1325377 Nodes

For the model display in the figure 3.2.7-43 a displacement of 1.7005 mm was measured when applying a force of 70KN. These results were obtained using refine mesh having 904040 elements. For that configuration, the simulation runs for several hours (if not day).

After several simulation with less refined mesh and observation of the deformed shape as well as the maximum and minimum constraints, it was decided to choose the model display in figure 3.2.7-38 having 227614 Elements and 354990 Nodes. The decrease of accuracy was then considered small compared to the simulation time difference.

If we consider the coarse mesh results in displacement of the XY symmetric 2 oblique model to be the reference value:

$$Error\ pourcentage = \frac{(Reference\ value - final\ value)}{Reference\ value} * 100 \quad (89)$$

$$Error\ pourcentage = \frac{(1.7138 - 1.7005)}{1.7138} * 100 = 0.7760\ \% \quad (90)$$

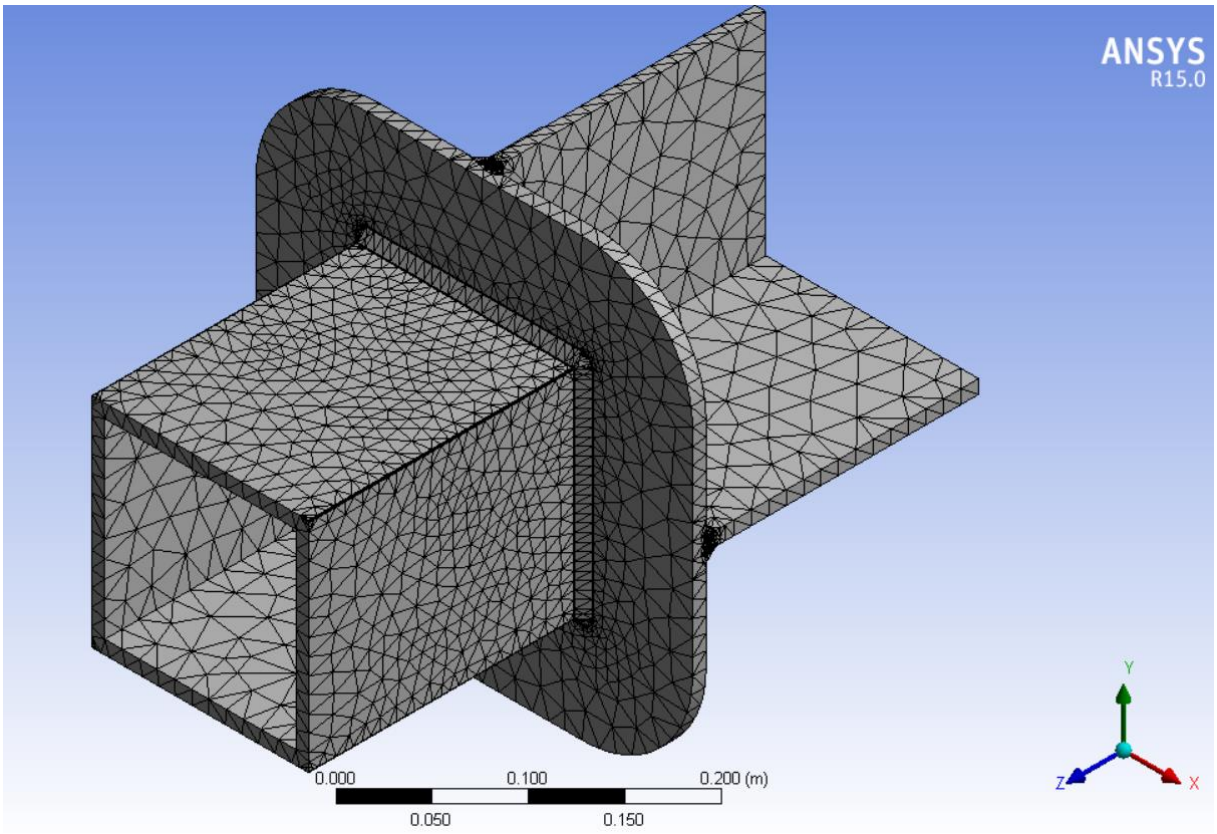

Figure 44: Coarse mesh model without reinforcements – 249981 Elements, 382907 Nodes

For the model display in the figure 3.2.7-44 a displacement of 2.3147 mm was measured when applying a force of 70KN. This result was obtained using coarse mesh having 249981 elements. For that configuration the simulation was run in a few minutes.

We logically obtain a displacement bigger than with the configuration having oblique reinforcements.

For this configuration, the same procedure was used in addition with a study of convergence of a model using the symmetry.

The obtained percentage of error, considering the coarse mesh model without symmetry along the ZY plan (figure 3.2.7-44) to be the reference, is:

$$Error\ pourcentage = \frac{(2.3147-2.3041)}{2.3147} * 100 = 0.4579\ \% \quad (91)$$

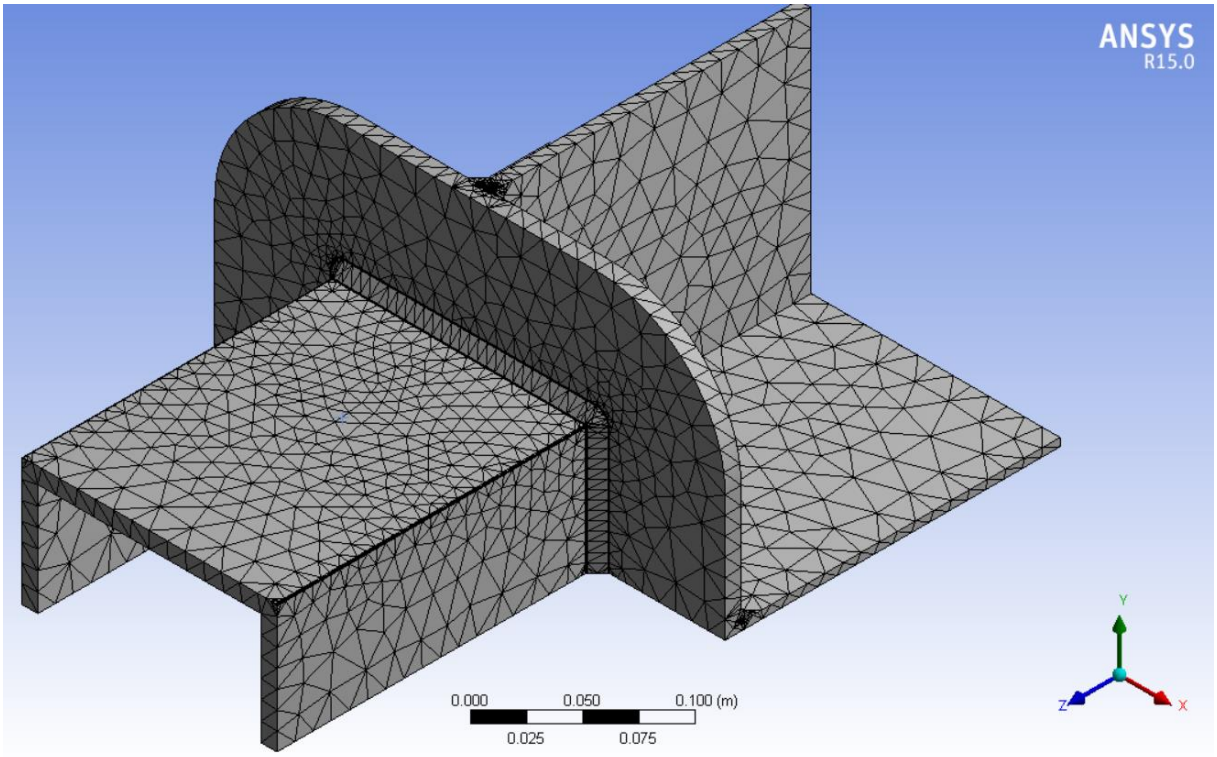

Figure 45: Coarse mesh symmetric model without reinforcements -130151 Elements, 200546 Nodes

For the model display in the figure 3.2.7-45 a displacement of 2.3041 mm was measured when applying a force of 70KN. This result was obtained using coarse mesh having 130151 elements. For that configuration the simulation was run in a few minutes.

According to our results, the symmetric model was validated and used for the others simulations.

As both the two and four oblique reinforcement configuration are built one the same principal (and from the same geometric model), only the two oblique reinforcement model was studied. It was assumed that the configuration with four should also produce a convergent mesh and valid results in displacement and constraint.

For our simulation the temperature reference was set to 22 °C, the analysis was performed in static condition. Only one iteration was performed using direct sparse solver with the default full Newton-Raphson nonlinear analysis running on two processors. This solver is known to be one of the most robust. We set the big displacement option to be inactive. We set stabilization option to constant and used the energy method with a dissipation ratio of 1.e-004 and a limit force stabilization of 0.2.

The elements used for the simulation are SOLID187 together with contact element CONTA 174, target element TARGE170, SURF154, COMBIN14. SOLID187 are the higher order 3-D, 10-node element having quadratic displacement behavior perfectly suited for CAD/CAM systems. The element is having three degrees of freedom at each node: translations in the nodal x, y, and z directions. The element allows to simulate plasticity, hyper elasticity, creep, stress stiffening, large deflection, and large strain.

3.3Results

3.3.1 Displacements

For the model we used a geometry defined as follow:

Deck thickness: x mm grade A

Flange: x mm grade A

Reinforcement platting: x mm grade A

Weld size: x mm

σ_e= 255 Mpa

σ_r=4.6 E8 Pa

C=x mm

Pillar thickness=x mm

In the following section, the FE results obtained with the model selected in 3.2.7 for one specific loading (20KN, X axial force plus additional bending moment) will be exposed. At the end of this section, a summary table of all the results will be displayed.

In the diagram display on figure 3.3.1-46, the deformation for the selected model -20KN, coarse mesh with quadratic elements, 2 oblique reinforcement- is 0.4906 mm in the X direction and situated as expected at the top of the pillar. The minimum displacement is not significant and situated at the bottom of the pillar.

It is possible to observe a bigger deformation of the deck in the Z direction at the place where there are no reinforcements and very small displacement on deck above the oblique reinforcements.

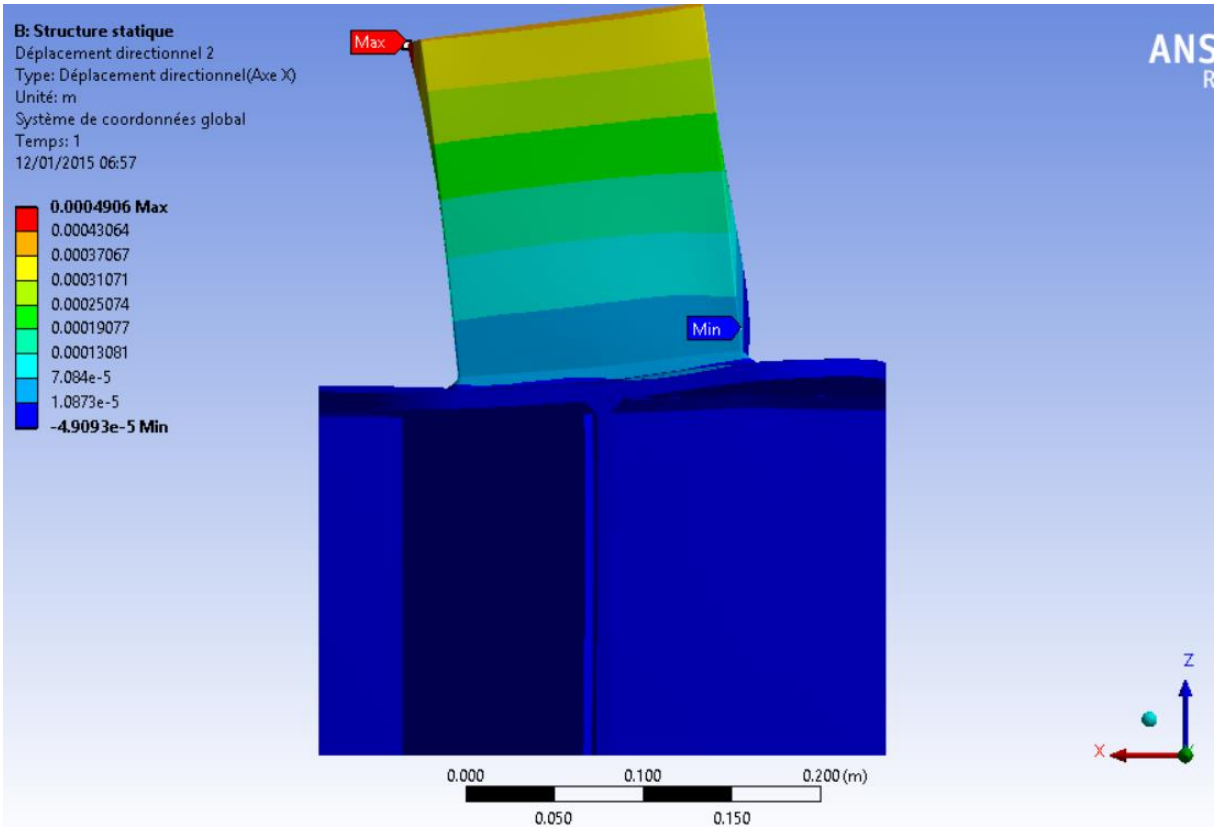

Figure 46: Deformed shape in X direction, 2 oblique, lateral view.

The following figure 3.3.1-47 displays the top view of the deformed shape in the X direction. A bending of both pillars faces positively along X-axis can be observed. This bending is resulting from the additional stiffness bring by the two other lateral faces -displayed in orange and yellow- during an axial X loading.

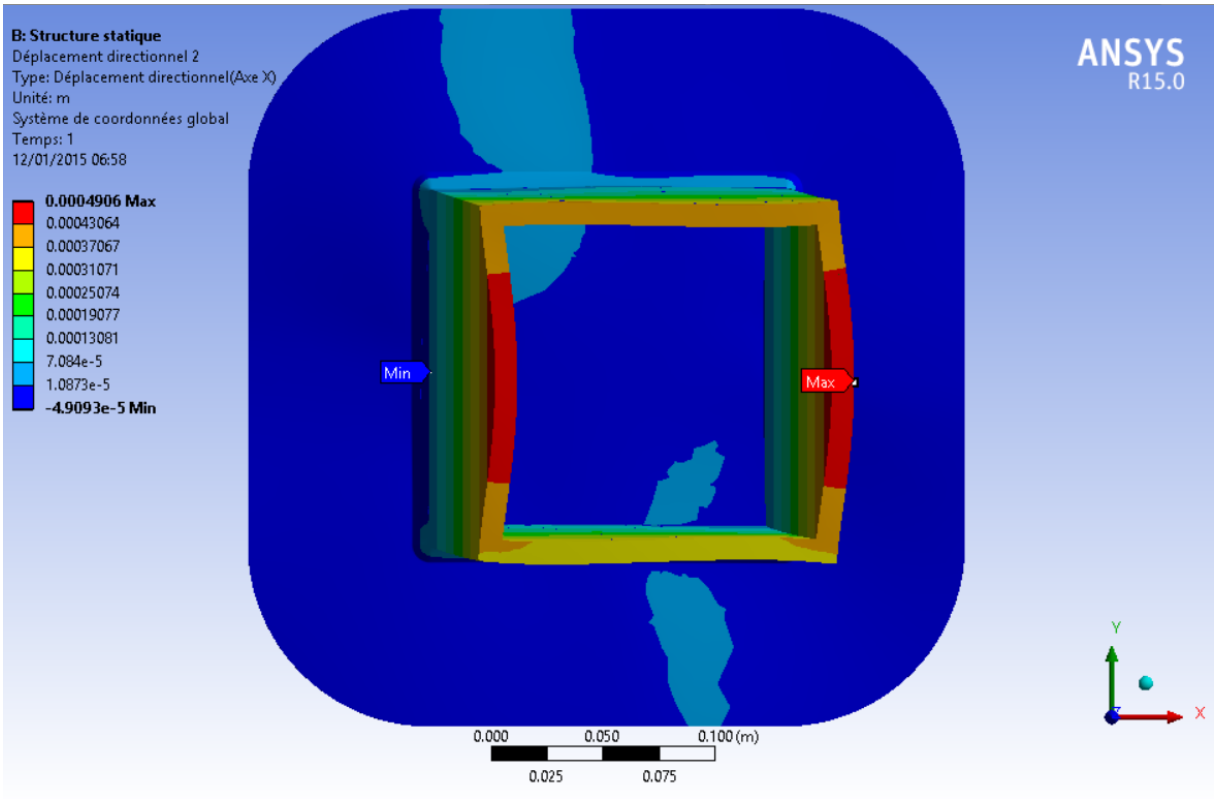

Figure 47: Deformed shape in X direction, 2 oblique, top view.

On the following figure 3.3.1-48; it is possible to clearly observe on the iso-view that the reinforcement platting is subjected to very few if not 0 displacement. This is coherent with what could be expected using the previously set boundary condition.

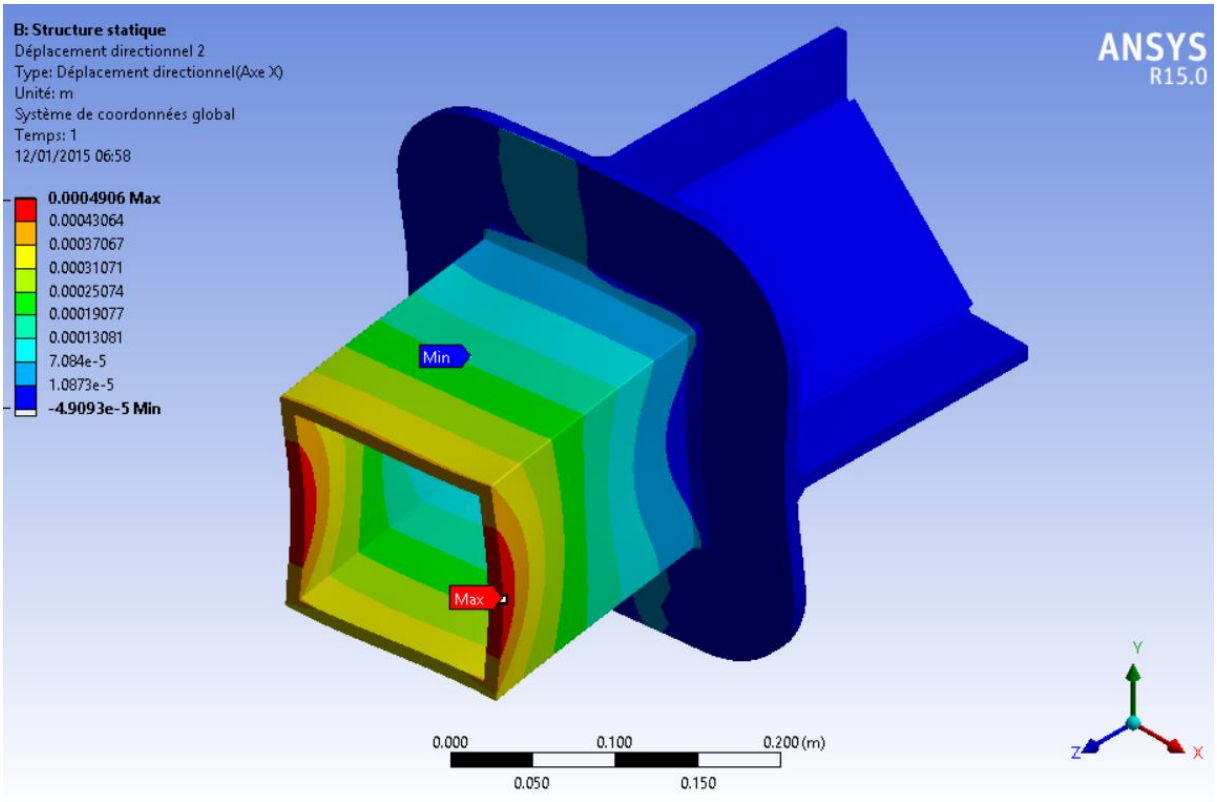

Figure 48: Deformed shape in X direction, 2 oblique, iso view.

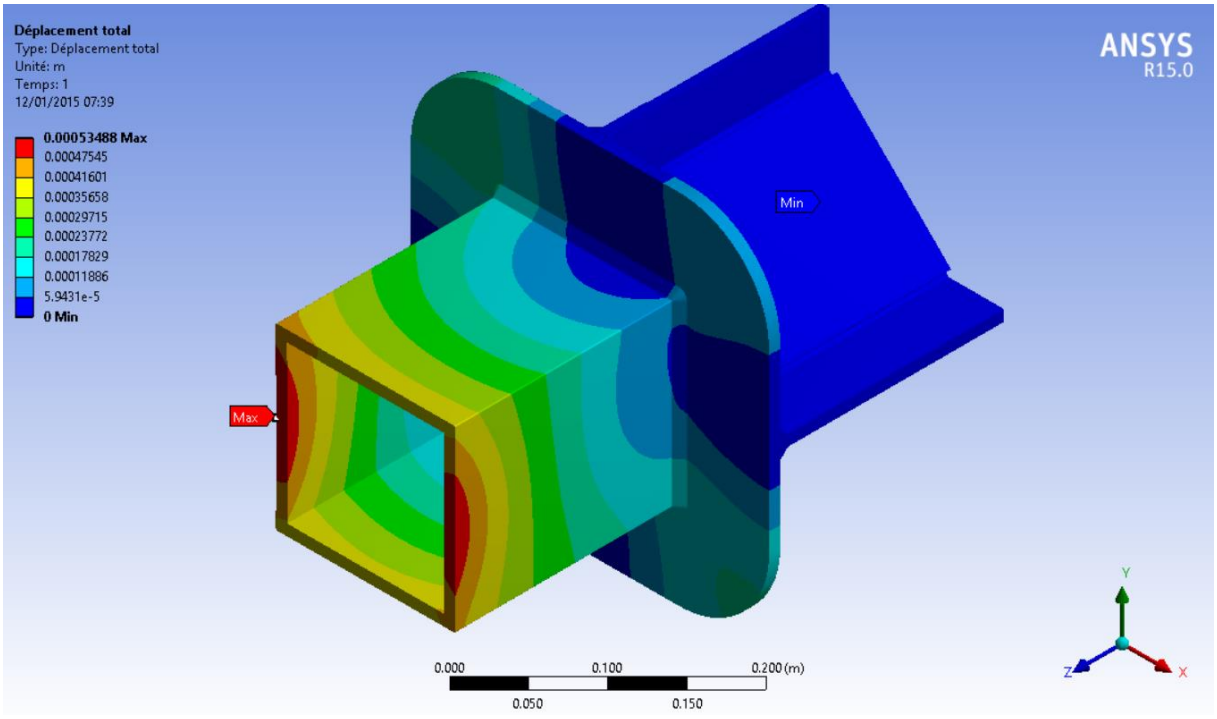

Figure 49: Total deformed shape, 2 oblique, iso view.

When looking at the total deformation in figure 3.3.1-49, the reader will observe that the bigger part of it is coming from the X displacement. As on the previous figure, very small

deformation in the oblique platting is observed. For 20KN, the maximum total deformation is about 0.53 mm on the top of the pillar.

Regarding the configuration without reinforcement on figure 3.3.1-50, a bigger deck deformation of 6.469 E-05 is measured instead of 1.0873 E-05 mm for the configuration with reinforcement. It is also possible to observe that the maximum deformation is 0.66361 mm, 26% more than the one obtain in the solution with reinforcement.

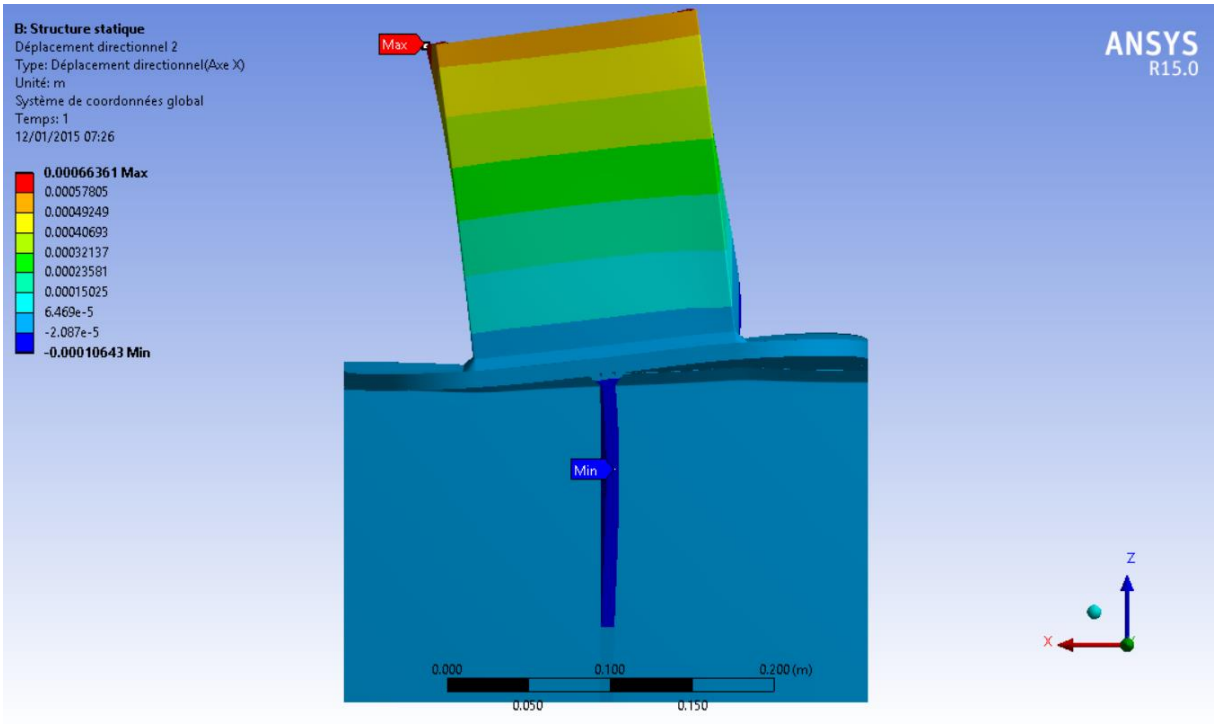

Figure 50: Deformed shape in X direction, not reinforced, lateral view.

On the top view figure 3.3.1-51, we observe that the deformed shape is globally the same the one obtain on the configuration with the two oblique reinforcements. A different scaling factor was used for both models with and without reinforcement (scaling factor of 62 for the reinforced configuration, 42 for the not reinforced one).

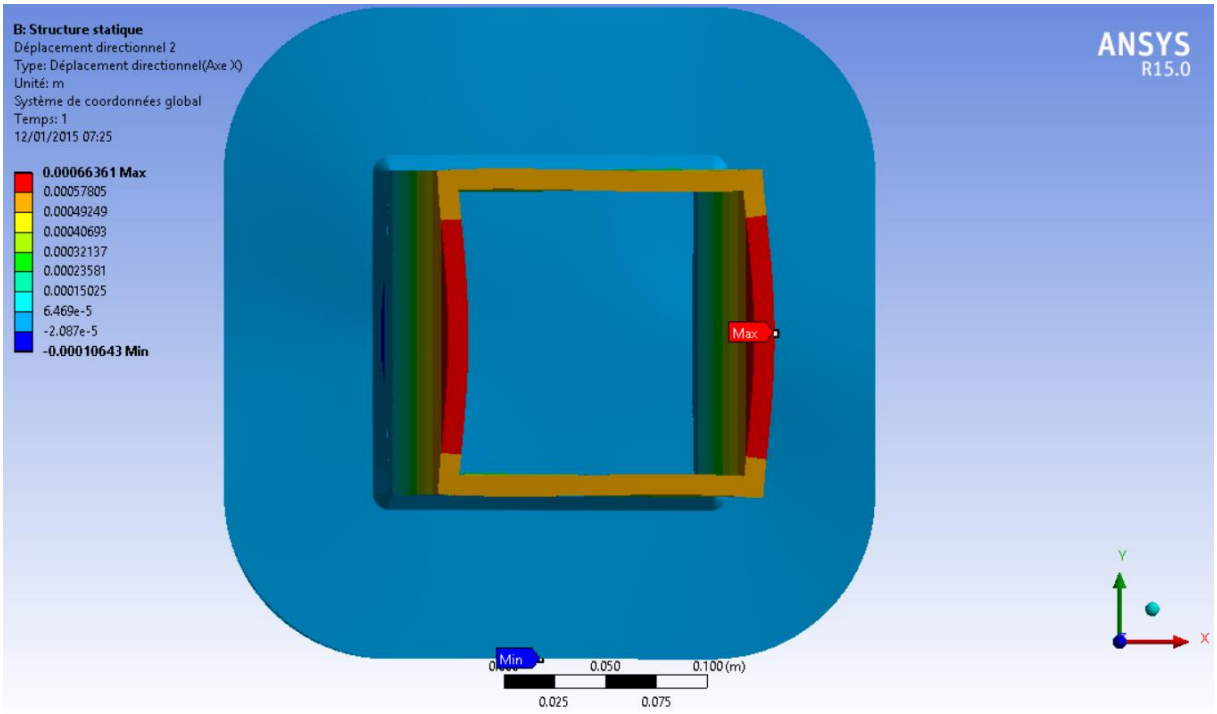

Figure 51: Deformed shape in X direction, not reinforced, top view.

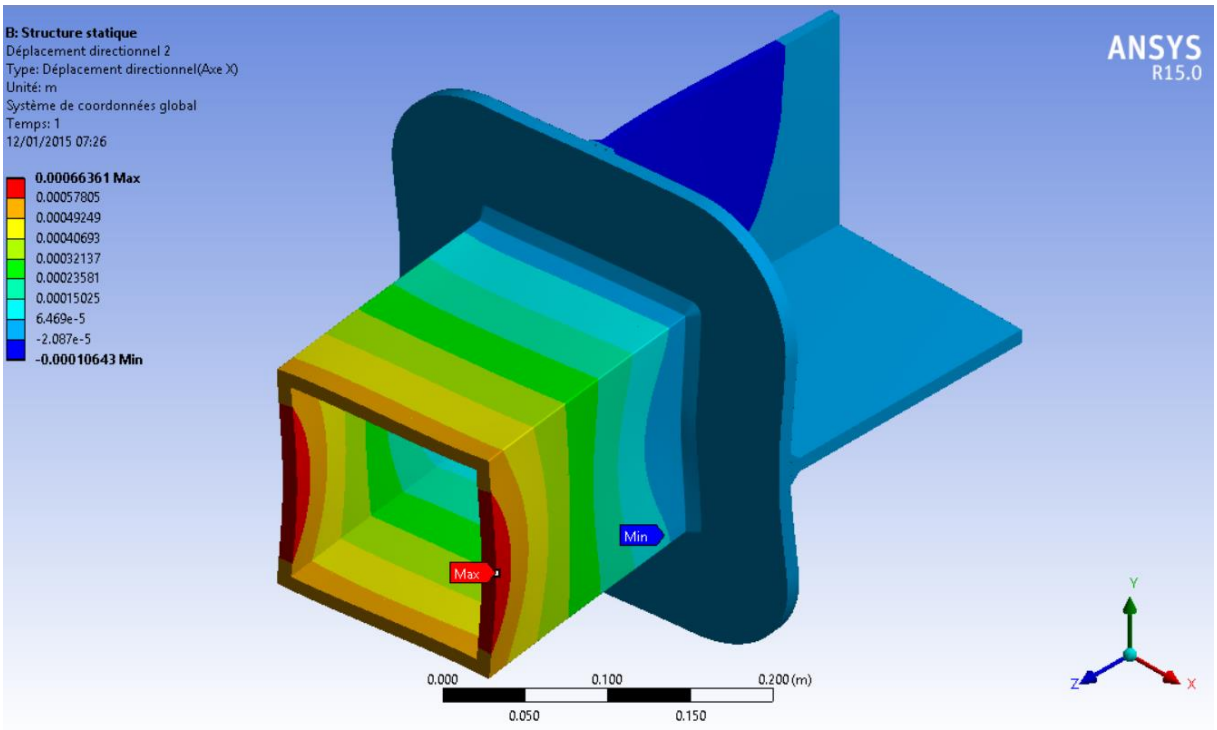

Figure 52: Deformed shape in X direction, not, iso view.

The iso view on figure 3.3.1-52 displays a deformed shape coherent 0 displacement in the X direction on the deck. This results will not be the same in the Z direction except above the girder and beam where it will be around 0 mm. But as the Z displacement are not as important

as the one along the X-axis, no display of it are done (they are of course include in the global displacement figure 3.3.1-53).

On the following figure 3.3.1-53, the total displacement is display. As expected, the beam and girder are having a displacement close to 0 mm. logically, the deck above beam and girder is also having a very small displacement that is around 0 mm. The maximum displacement, around 0.70343 is measured at the top of the pillar.

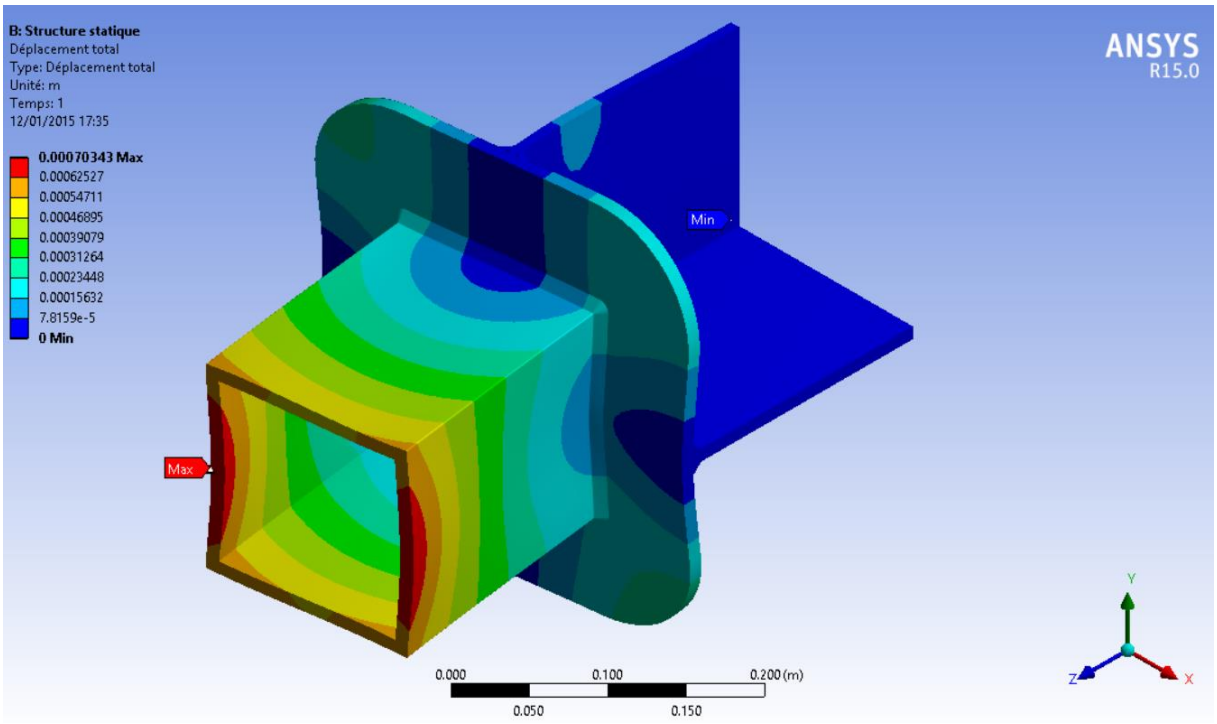

Figure 53: Total deformed shape, not reinforced, iso view.

On the following figure 3.3.1-54 of the pillar after breaking, it is possible to observe that the pillar is having a maximum displacement on the opposite side of the face. It is on this face that the loading was apply. A minimum displacement is observe on the face submitted to compression.

Figure 54: Pillar with 2 oblique reinforcement after breaking: 97.5 KN apply load © STX France

3.3.2 Stress

On the following section the author will be studying the constraints on the assembly. As the one used by STX are the intermediate principal one, the author studied particularly this constraints.

As displayed in the figure 3.3.2-55 -the not reinforced case- the maximum intermediate constraint is equal to 6.5738E8 Pa when the system is subjected to a 20KN X axial loading and an additional bending moment of 15200N.m. The maximum stress appears to be on the surrounding of the defect modeling at the weld's root. The minimum one is at the opposite root and resulting from compression. The maximum constraint is acting in only a few numbers of elements and is decreasing very fast for the surrounding element. Only elements having a constraint superior to 5.2043E7 Pa are displayed.

Mechanically this results is easy to understand, a moment along Y axis is created around the weld center of inertia when the weld is subjected to traction after the axial loading as explain on the figure 3.3.2-56.

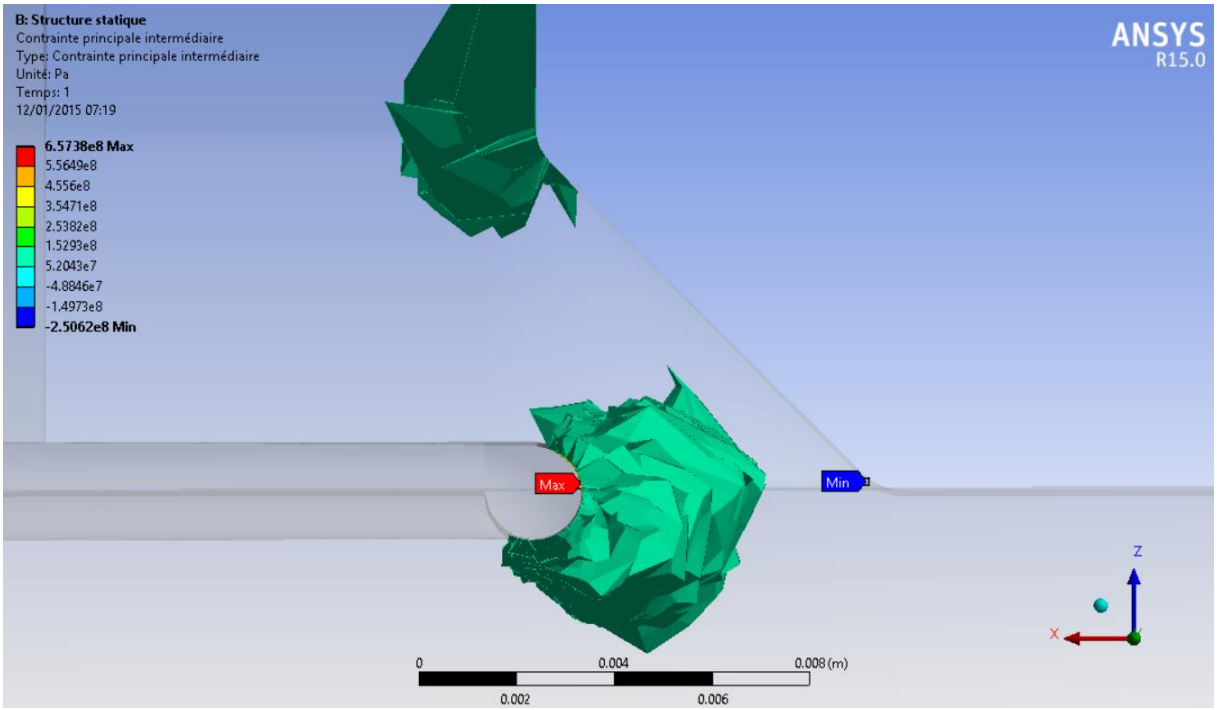

Figure 55: Zoom on maximum and minimum constraint on root weld. No reinforcement.

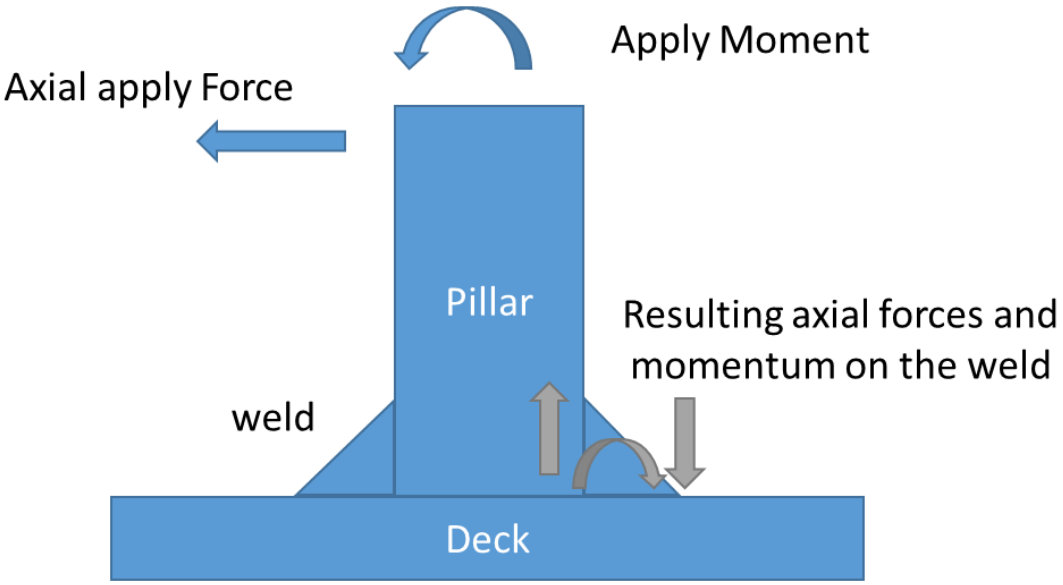

Figure 56: Explanation of the reactions forces on the model

On the figure 3.3.2-57, the maximum intermediate constraint is display. As explain above, this maximum constraint appears to be on the defect modeling just on top of the beam. This maximum constraints is having acting only locally, as we will see on figure 3.3.2-58, the majority of the model is subjected to a constraint that is less than 5.2043E7 Pa.

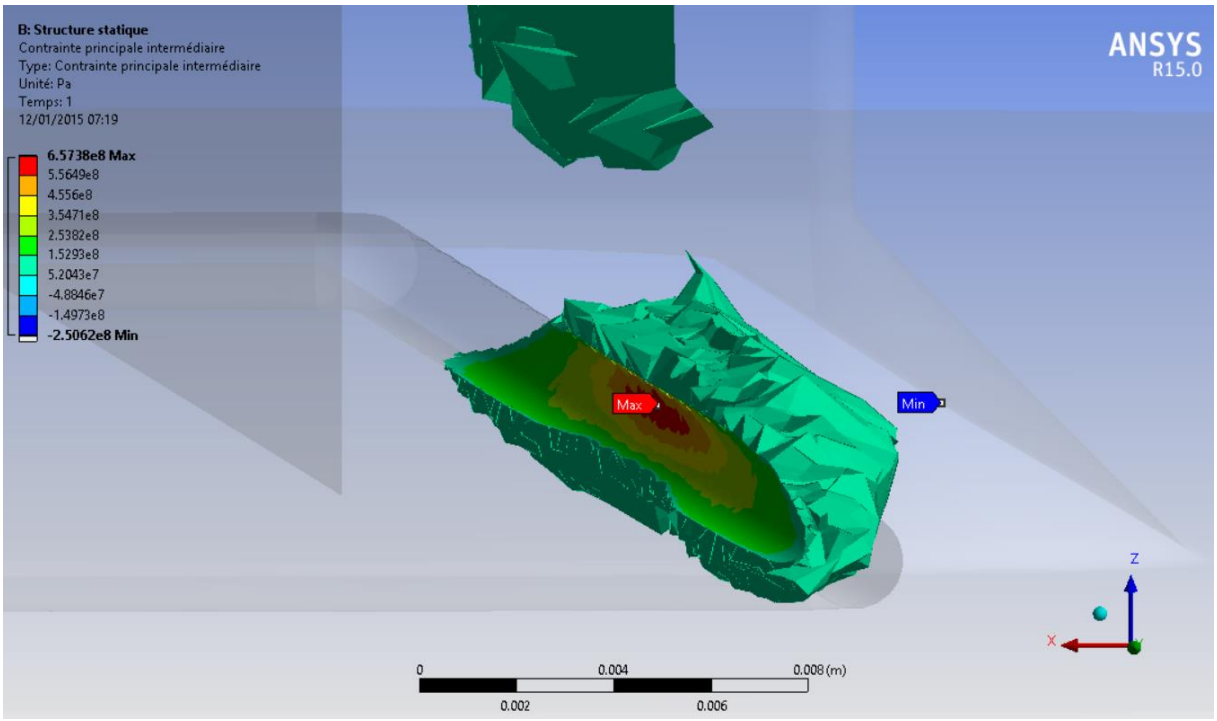

Figure 57: Zoom on maximum and minimum constraint on root weld. No reinforcement.

On the figure 3.3.2-58, only elements having a constraint superior to 5.2043E7 Pa are display. The simulation was made with 20KN axial loading and additional bending moment. The configuration is without reinforcement.

On the figure 3.3.2-58, the comportment of the maximum constraint appears to be acting locally only. The majority of the models being subjected to a constraint less than 5.2043E7 Pa. Only elements having a constraint superior to 5.2043E7 Pa are displayed. The configuration is without reinforcement.

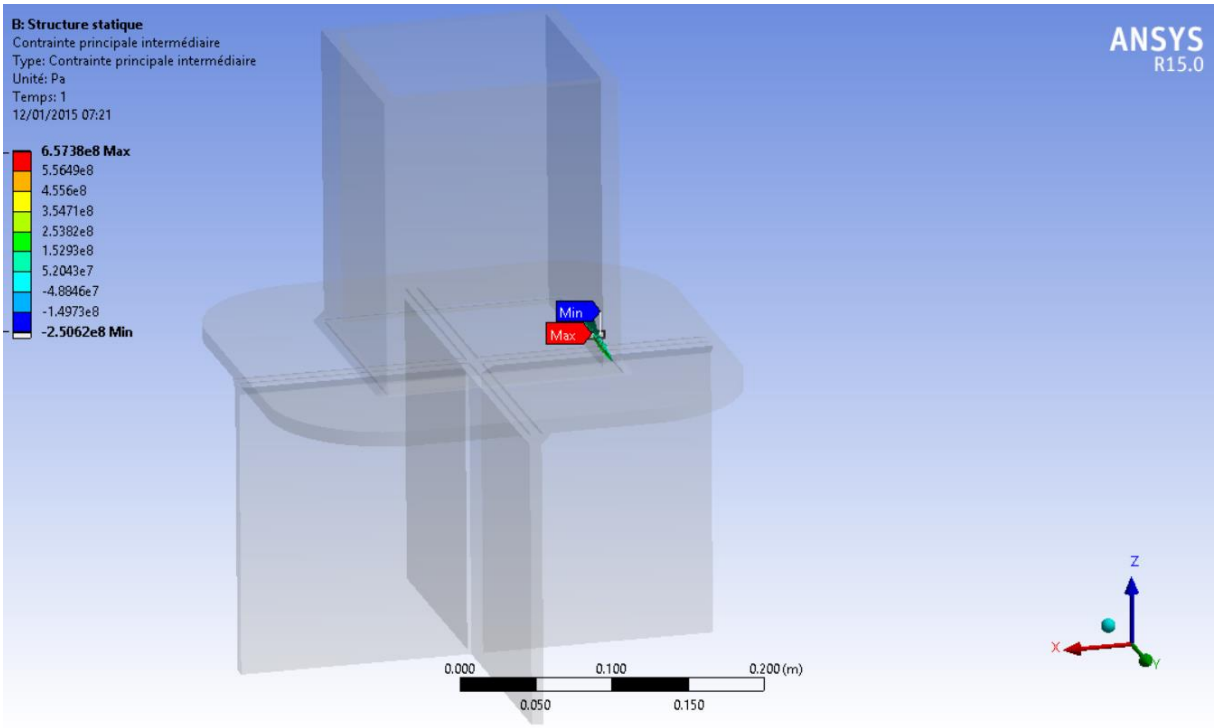

Figure 58: Global view of the model. Solution without reinforcement.

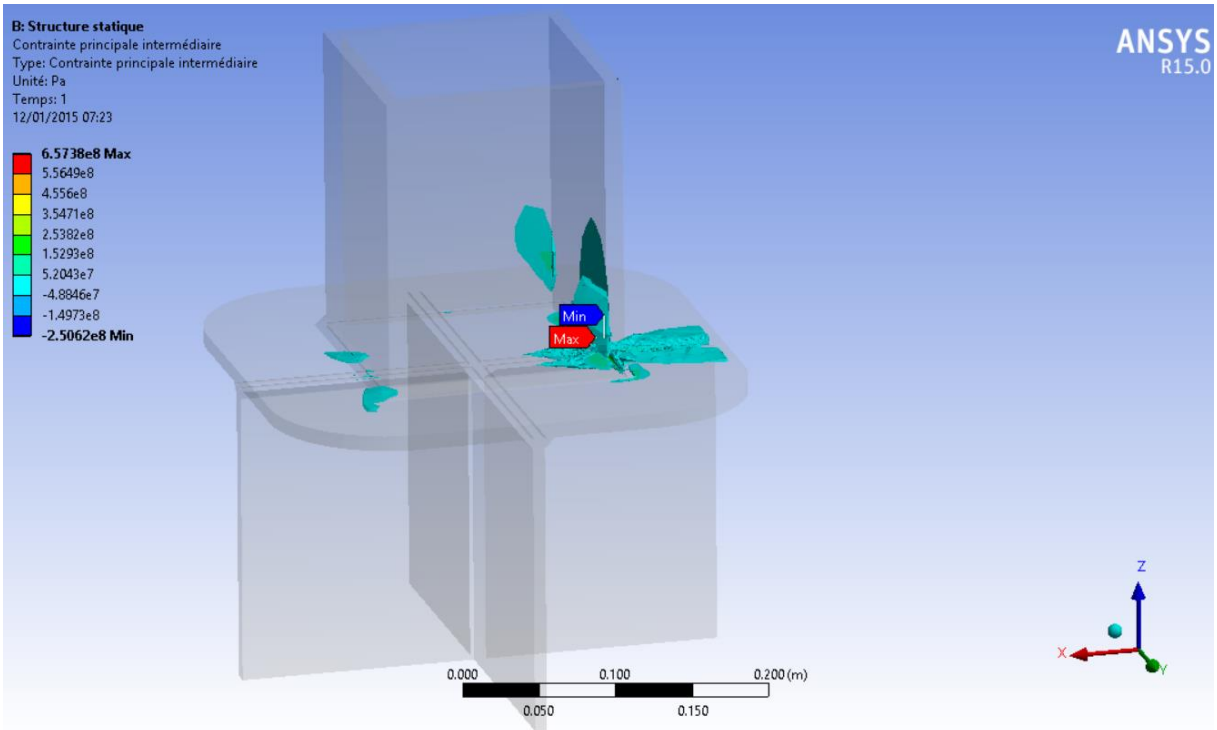

Figure 59: Global view of the model. Solution without reinforcement.

On above figure 3.3.2-59 only element having an intermediate constraint superior to 3.99E7 Pa are display. This shows again that the constraint is acting only locally. The majority of the

models having a constraint of 0 Pa. The simulation was made using same loading and model than on used in figure 3.3.2-59.

One the following paragraph the results obtain using the model for 2 oblique reinforcement will be presented.

As it can be seen on the figure 3.3.2-60, the maximum intermediate constraint is obtained for approximately the same position than for the simulation without reinforcement. Here the maximum stress is about 4.9446E8 Pa that is less than on the version without reinforcement. A decrease of 24% of the maximum intermediate constraint is observed using 2 oblique reinforcement.

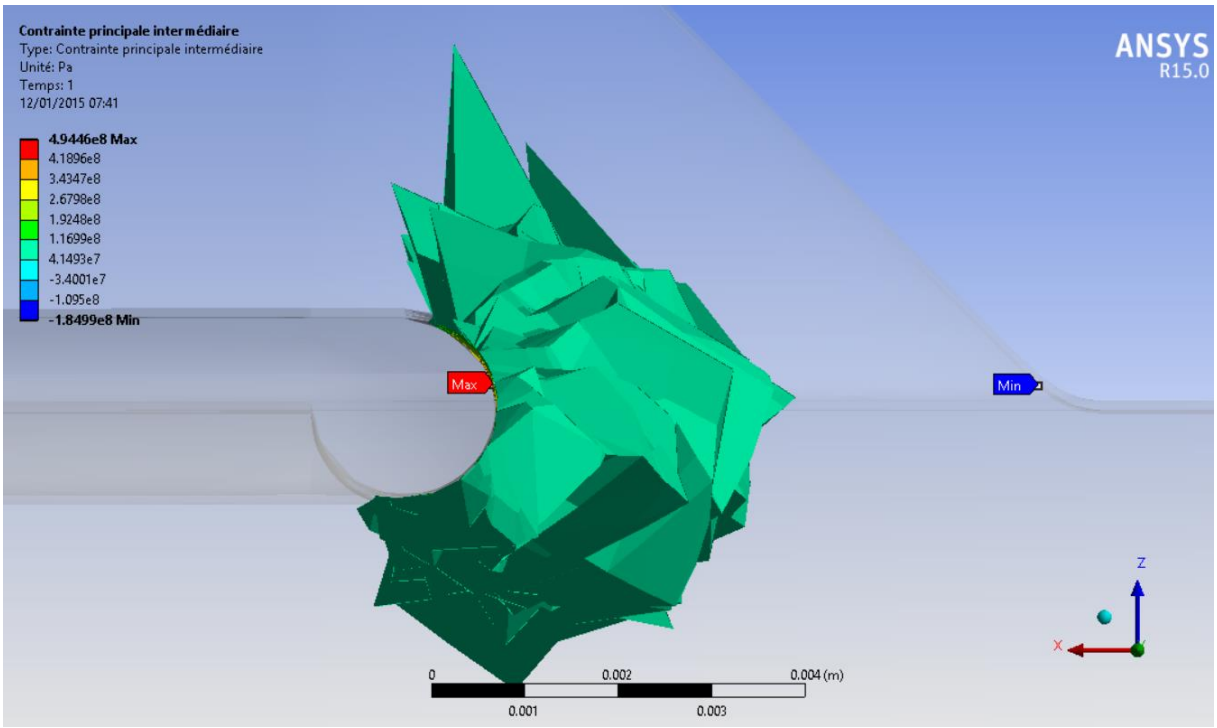

Figure 60: Maximum and minimum constraint on root weld. Solution with 2 oblique.

Again, it is possible to observe on figures 3.3.2-61-62 a concentration of constraints and fast decrease of constraints for the surrounding elements. The maximum constraint is obtained on top of the beam. Only elements having a constraint superior to 4.1493E7 Pa are displayed. The simulation was made using the same loading and model than the one used in figure 3.3.2-60.

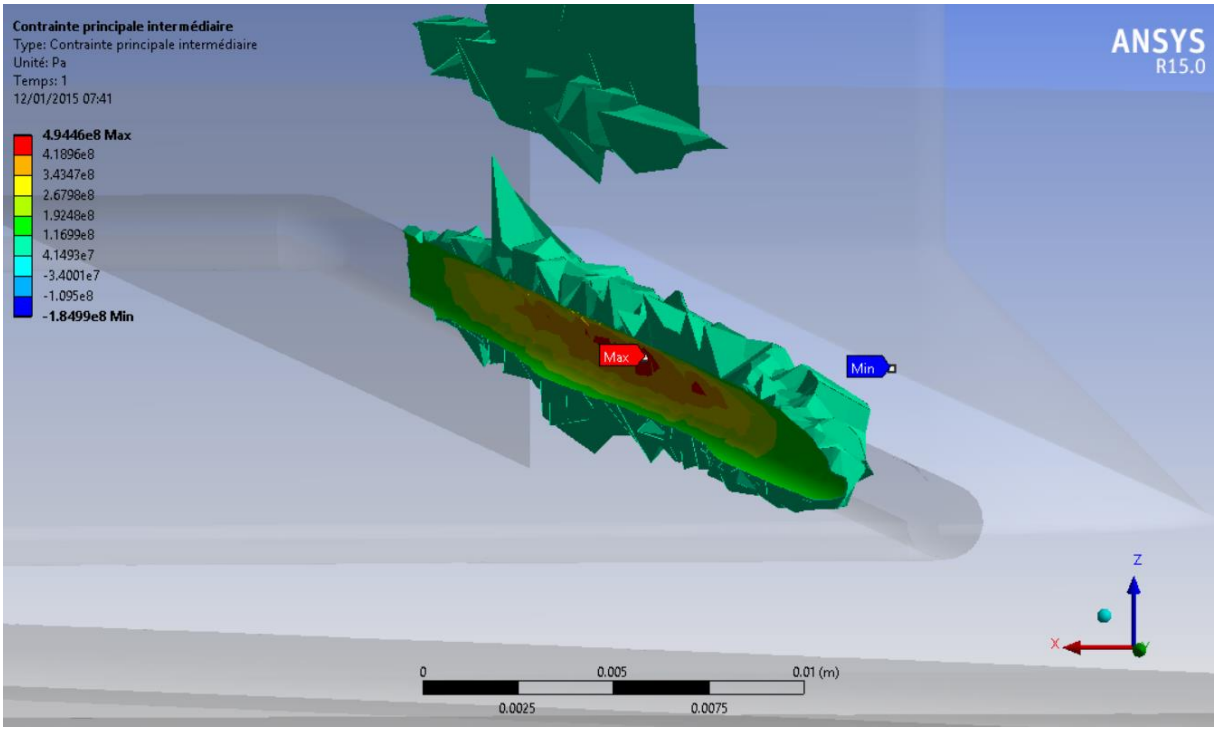

Figure 61: Zoom on maximum and minimum constraint on root weld. Solution with 2 oblique.

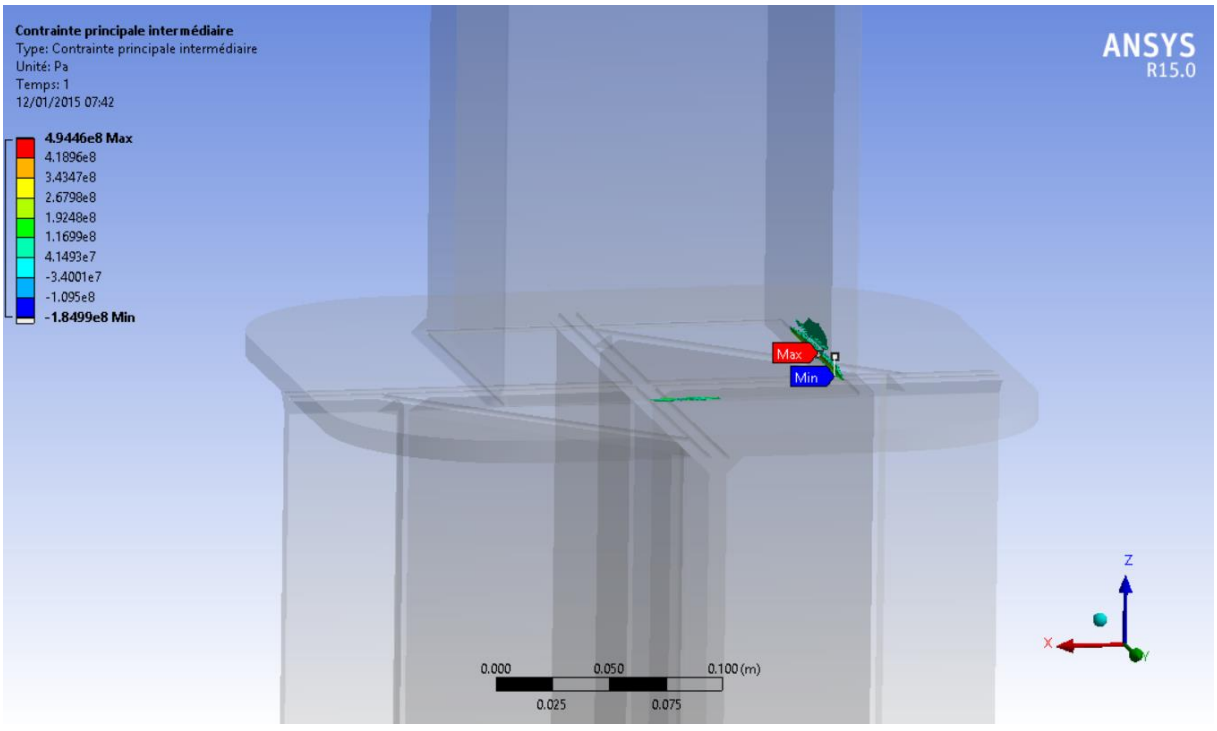

Figure 62: Global view of the model. Solution with 2 oblique.

On figures 3.3.2-71-64, only element having a constraint superior to 3.24E7 Pa are display. The loading is the same than the one previously used.

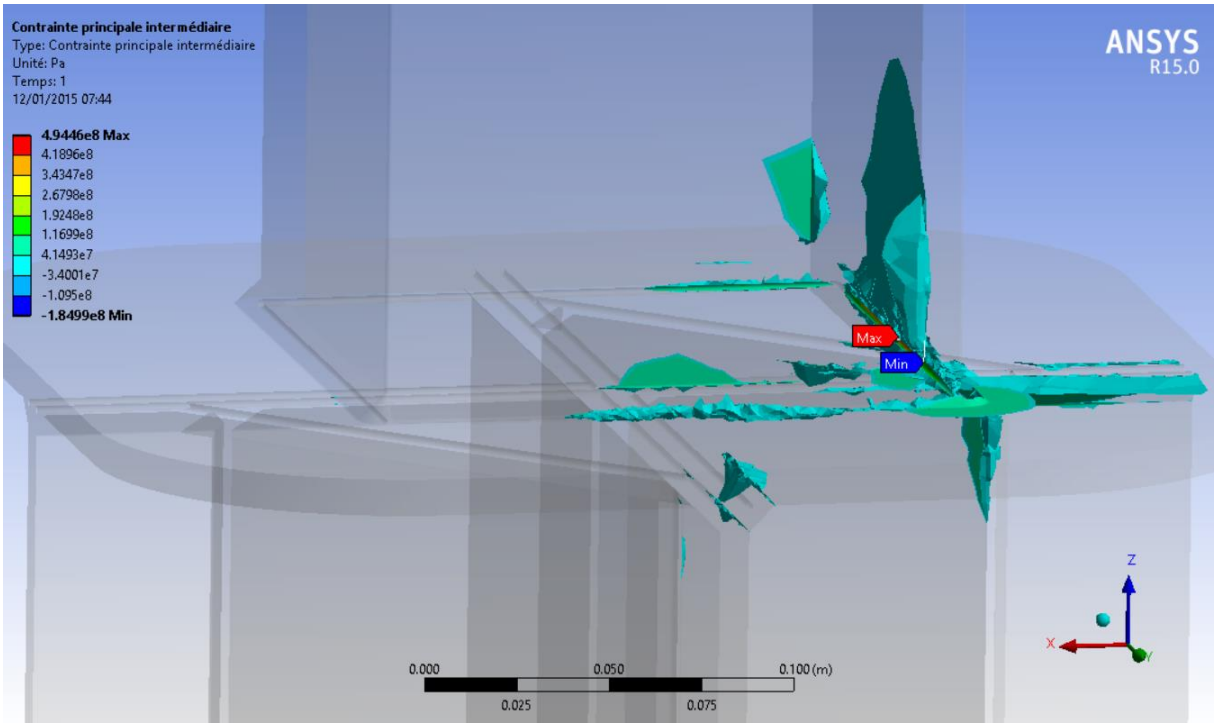

Figure 63: Global view of the model. Solution with 2 oblique.

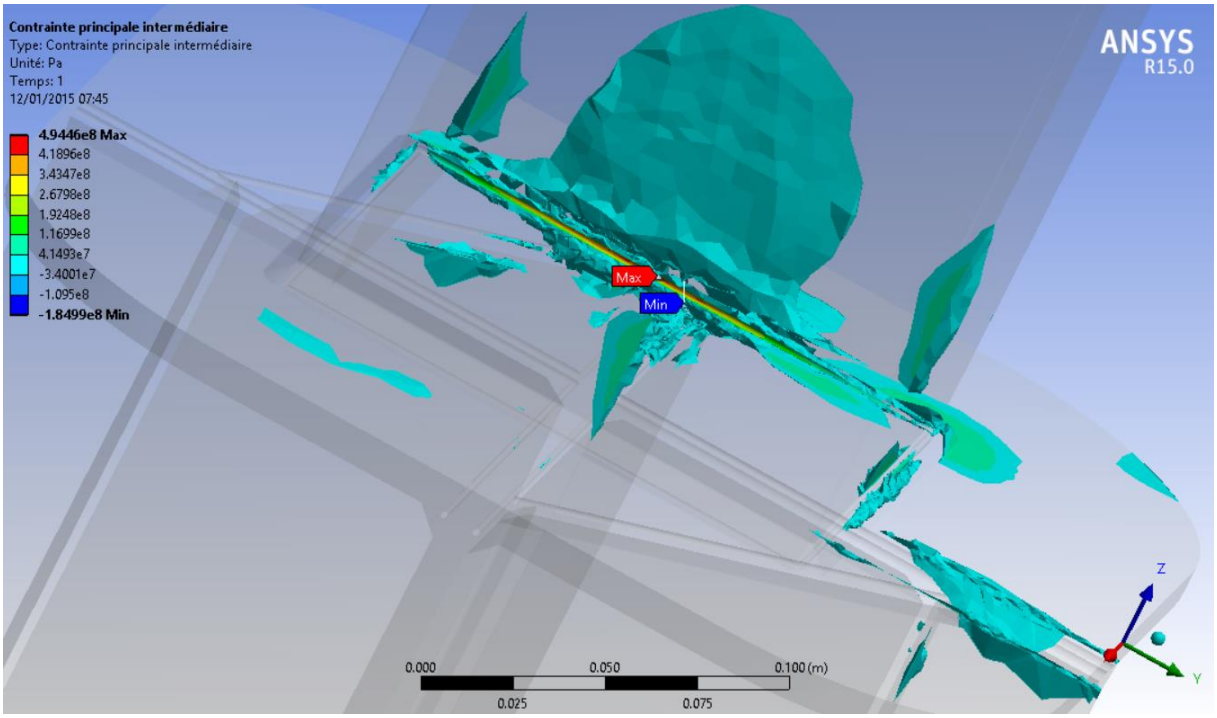

Figure 64: Global view of the model. Solution with 2 oblique.

Table 7: Displacements and intermediate principal constraints in both configuration

Loading [KN]	Without reinforcement		With 2 oblique reinforcement	
	Displacement along X [mm]	Maximum intermediate Constrainte [Pa]	Displacement along X [mm]	Maximum intermediate Constrainte [Pa]
0	0	0	0	0
20	0.66361	6.57E+08	0.4906	4.94E+08
40	1.3247	1.31E+09	0.98021	9.89E+08
70	2.3147	2.30E+09	1.7005	1.68E+09
100	3.296	3.28E+09	2.4469	2.47E+09

On the table 3.3.2-7 a summary of the results obtained in displacement and intermediate constraint is given with the relative loading.

It is easy to observe that both constraints (figure 3.3.2-65) and displacements (figure 3.3.2-66) are linear even after crossing the elasticity limit set at 2.5E8 Pa. The same linearity is observed even passing the critical stress of 4.6E8 Pa.

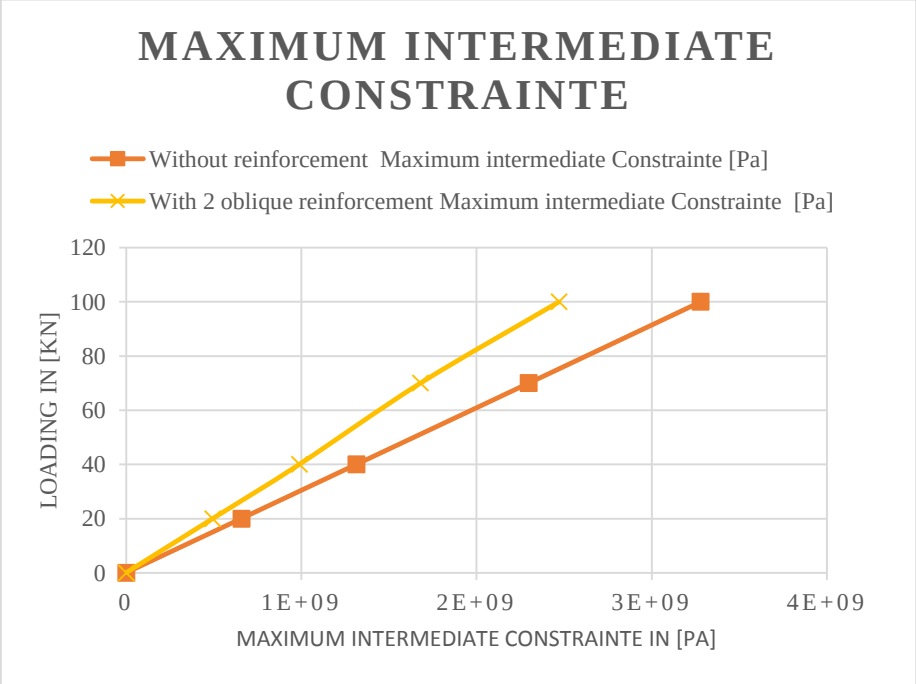

Figure 65: Maximum intermediate constraint, with and without reinforcement.

Logically, the constraints on the assembly are superior without any reinforcement. On the previous figure 3.3.2-65, the resulting stress calculated at 40KN loading (plus additional moment) is around 1E09 Pa for the solution with two oblique reinforcement. On the configuration without any reinforcement and using the same loading, a constraint of 1.31E9 Pa was calculated.

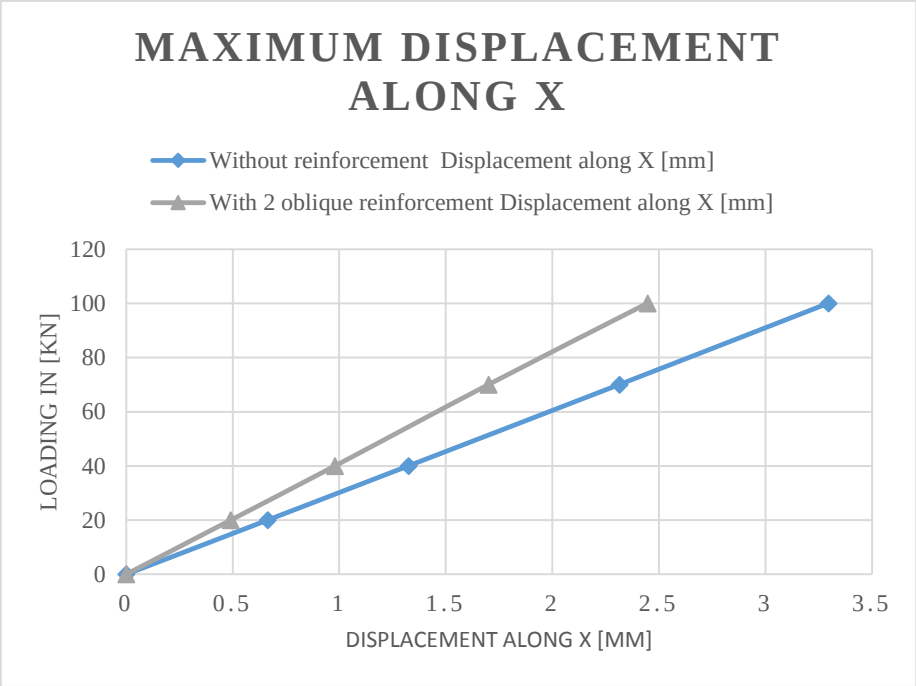

Figure 66: Maximum displacement along X axis, with and without reinforcement.

Again, the displacements on the assembly are superior without any reinforcement. On the previous figure 3.3.2-66, the resulting displacements calculated at 40KN loading (plus additional moment) are around 0.98mm for the solution with two oblique reinforcement. On the configuration without any reinforcement and using the same loading, a displacement of 1.32mm was calculated.

This shows that the reinforcement is decreasing the displacements along X of the system. As the X displacement are the one having the biggest influence on the global displacement, the reinforcement globally positively reduce the displacement and the intermediate principal constraint.

3.4Verification and Validation

3.4.1 Convergence Study

Convergence study is part of the V&V process in any FE analysis. As this study was developed in 3.2.7, the author will not consider it in this part of the thesis.

3.4.2 Comparison with Hand Calculation

In order to be able to compare the FE results with the hand calculation, the author used the manual excel sheet. Then, entering the same geometry than the tested one in the geometry parameter field allow to look at the obtain stresses (see section 3.1: tool presentation). The VBA macro was also forced to make a loop on only 5mm weld throat size. For the loading, we apply a moment corresponding to the one obtain at the foot of the pillar in order to be coherent with the laboratory experiment. No axial loading where applied as the Excel was designed only for vertical tension/compression + Moment and not for axial loading.

The following table 3.4.2-8 is giving an overview of the obtained results in constraint. Unfortunately, no comparisons are available in displacement for the analytical solution.

Table 8: Real constraint obtained with excel manual program.

Loading [KN]	**Without reinforcement**	**With 2 oblique reinforcement**
	Maximum stress [Pa]	**Maximum stress [Pa]**
0	**0**	**0**
20	**2.53E+08**	**1.59E+08**
40	5.05E+08	3.18E+08
70	**8.84E+08**	**5.57E+08**
100	1.26E+09	7.96E+08

The following figure 3.4.2-67 is showing the linearity of the obtained results using the VBA code. But, as we can observe on the previous table, the solution without reinforcement is having a maximum stress above the elasticity limit define for the material and set to 2.3E8 Pa as soon as a load of 20KN is apply. For the reinforcement case, this limit is crossed between 20KN and 40 KN.

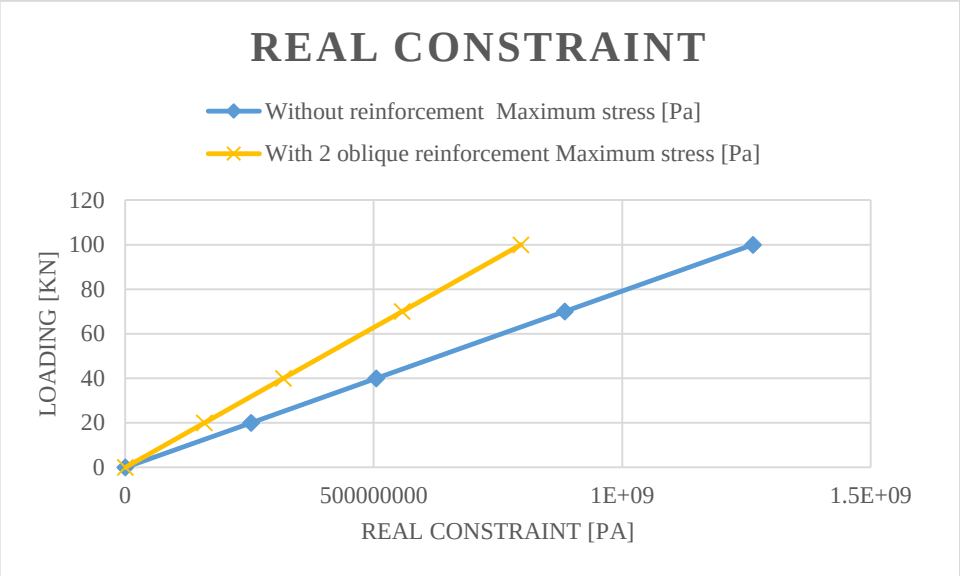

Figure 67: Constraint obtain using the excel sheet, with and without reinforcement.

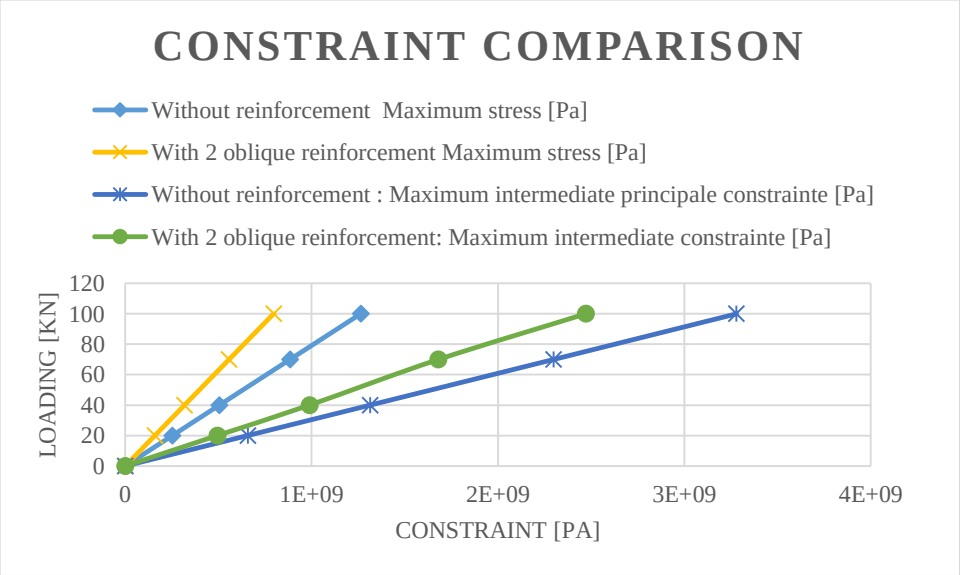

Figure 68: Comparative graph of the constraint - excel / FE - , with and without reinforcement.

The stresses obtained with the Excel sheet are about a half of the one obtained with the FE model. This could be due to the missing axial loading in the Excel, as only a reaction moment seen from the pillar bottom was apply. The Results obtained using the Excel are around 61% lower for the solution without reinforcement and around 67% for the reinforced configuration. In proportion, the axial loading is equivalent to approximately 51% of the total reaction forces (axial reaction forces + reaction moment) at the pillar bottom.

3.4.3 Comparison with Laboratory Test

3.4.3.1 Model Test

Unfortunately, the welds used during the experiments could not easily been measured and no precise record of it was available to for author. It also appeared that some measurement (displacement) could not be perfectly accurately performed during the laboratory test. Material data such as elastic limit was not easily accessible. These tests have been performed in 2011 at STX facilities. Several pillars were produced using different types of reinforcements and geometry. Then a lateral Tension force was applied at 0.96 m from the deck and the resulting displacements were observed at 0.2 m from the deck.

The model that we will study in the following is the one used for the FE analysis and in the Excel such as:

Deck thickness: x mm grade A,
Flange: x mm grade A,
Reinforcement platting: x mm grade A
Weld size: x mm
σ_e= 235 Mpa

The following diagram is an extract from the laboratory test results showing the organization of the test.

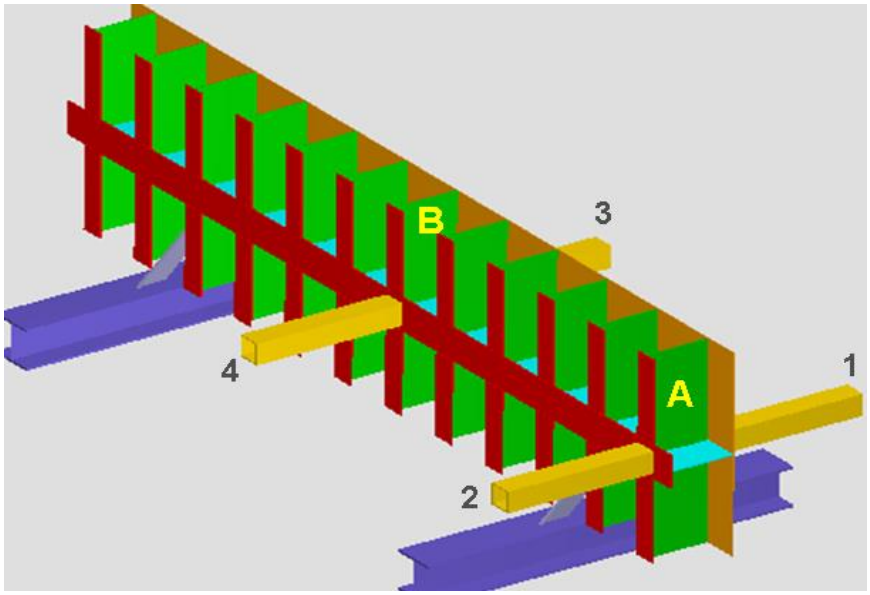

Figure 69: Model of the laboratory test © STX France

The pillar studied is the number 4.

3.4.3.2 Constraint and Displacement Comparison

To remind the reader about the displacement obtained with the FE model, the results obtained and plotted in the figure 3.3.2-66 are display again.

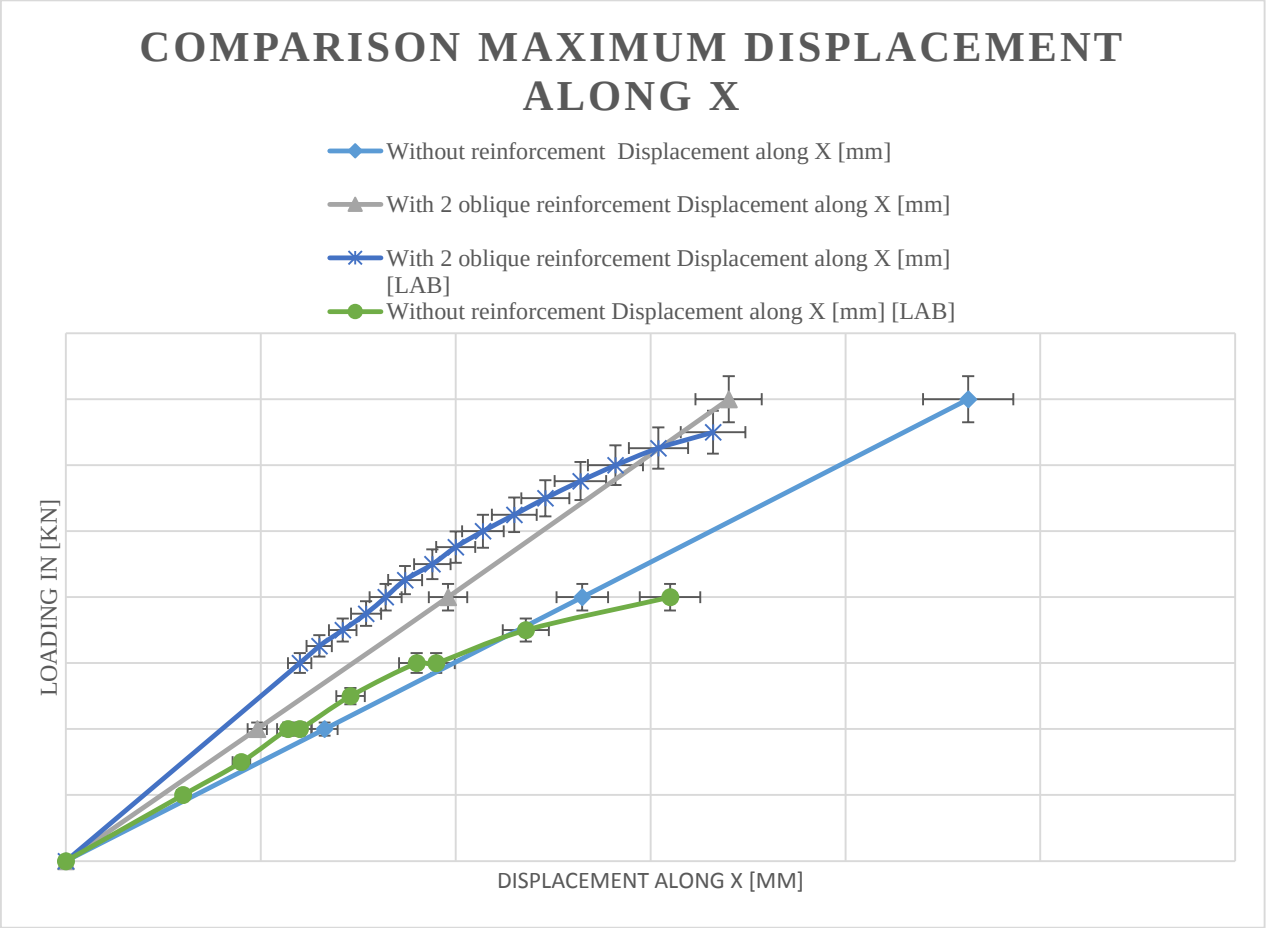

Figure 70: Comparison between laboratory and FE analysis displacement, with and without reinforcement, including 5% error margin.

Table 9: Obtained values during the test for the 2 oblique reinforcement configuration.
Confidential

Table 10: Obtained values during the test for the configuration without reinforcement
Confidential

Using the trend line plotting with a linear approximation for our constraint FE results, we obtain the following equation for the maximum intermediate principal constraint:

For the configuration with 2 oblique reinforcements:

$$y = 4e - 08.x + 0.0609 \quad (92)$$

With:

y = apply axial load for the solution with two oblique reinforcement in KN

x = Maximum intermediate principal constraint for the solution with two oblique reinforcement in Pa

$$\text{So for } \sigma = 235Mpa; y = 9.4609\ KN \quad (93)$$

For the configuration without reinforcement:

$$y_1 = 3e - 08.x_1 + 0.0396 \quad (94)$$

$$\text{So for } \sigma_1 = 235Mpa; y_1 = 7.0896\ KN \quad (95)$$

With:

y_1 = apply axial load for the solution without reinforcement in KN

x_1 = Maximum intermediate principal constraint for the solution without reinforcement in Pa

We clearly observe that for our FE model, the apply load needed to reach the elastic limit of 235 MPa are lower than the one obtain experimentally.

In the case of the reinforced configuration:

$$\text{For finite element model: } F_{ef} = 9.4609KN \quad (96)$$

$$\text{For the laboratory model: } F_L = 22.2KN \quad (97)$$

For the configuration without any reinforcement:

$$\text{For finite element model: } F_{ef1} = 7.0896KN \quad (98)$$

$$\text{For the laboratory model: } F_{L1} = 20.08KN \quad (99)$$

After analyzing more precisely the results during the verification process, it clearly appears that the finite element model is entering the plastic field even at the first simulation (20KN) for both cases - with and without reinforcement model-. These results seem to be the consequence of a highly local constraint area on the welds defect modeling.

Regarding the displacement results, the model does not provide with none linear results. A better setting of the simulation parameters could solve this in the future.

In appendixes the results of the laboratory tests will be displayed for both configuration.

Following the V&V process and after FE model verification using the laboratory tests, it is not possible to validate the FE model. However, some possibilities of improvement are available such as defect modification. Increasing the defect radius could result in a decrease of the local constraint. Otherwise, simplification of the model using direct contact between the pillars and deck and the adequate contact elements could also offers accurate results.

4. IMPROVEMENT PROPOSALS AND CONCLUSION

4.1Particular Case

It appears that due to the input ANSYS data, some cases could not be treated. For example, when a pillar is not exactly vertical but oblique, the acting forces are set to 0. By modifying the ANSYS macro used to input the FEM forces acting on the pillars, these cases could be studied. It will also be necessary to write a new code taking into account the angle of the pillars regarding the vertical axis in order to compute the new cross section area used to compute the moment of inertia.

4.2Link with Production

Knowing the type of reinforcement that are the most used in one project and the price of each of them in terms of material and welding time, it could now be possible to make production choices. Using statistics of the complete listing, the choice could be made to increase locally the deck size or to increase the reinforcement plate size in order to avoid a bigger reinforcement, which could be more costly to produce; or the opposite, to reduce deck or plate reinforcement size but using a stronger reinforcement type. These choices will be linked to the weight and so directly correlated to the final cost.

Making a direct loop from the Excel listing results into the local ANSYS workbench model will allow to easily quantify the total weight of each reinforcement.

Then, in order to decompose the different subsystem of the assembly and to have a good understanding of the weight of each of them, it is also possible to write a small routine computing the different plate's areas. This will then help for the plates cutting and again to get a better estimation of the final cost. It will then of course be useful to use a software for cutting optimization in order to arrange all the reinforcement plate areas in an optimize way. By assigning a particular material type to the weld it will also be possible to quantify the welding wire needed in total.

In addition, this loop could also help to validate every reinforcement's proposition from the Excel regarding the admissible stress. But it have to be noticed that this process could be extremely time consuming using FE and probably not fully useful. (Validation of only a set of reinforcement well chosen could be more suitable).

All this together could help to better define a project price regarding this particulars field of interest and so to make an offer matching production and customer requirements as close as possible.

In the future, a study of the industrialization process will be performed. With the data extract from the 3D model, the best reinforcement could be chosen knowing the influence in terms of prices (time to produce, material, weight…) as explained above.

It could perhaps also be interesting to include the deformation and constraints induced by the welding process. As lots of research papers were published on this subject this last years. Including also new welding process could help to reduce the influence of the welding defects.

The author also proposes to study the influence of a zero defect FE model, in order to quantify whether this zero defect model could be sufficient for the hull department.

As today the computation power available is increasing, it was possible to design a solid model for the local pillars model without too many trouble, later, using symmetries it should become possible to enter the solid field for the full scale model. This model could then be including the pillars. Ideally, this global solid model could also be updated at each modification and globally or locally recomputed in a parametric way. This could help to synchronize the different naval architecture teams during the design loop. As per now, no comparison are available between a global solid and a global shell model, the interest of doing so is not that obvious and could result in a lack of time instead of a money gain.

These make this stage for big passenger ship still very far from our concerns.

4.3 Parameters

For now only weld size and type of reinforcement were optimize. Platting size could also be included as a parameter. In a second time, if a loop is made on the global model, the pillars scantling could also be define as parameter.

Another parameter to be considered is the number of reinforcement in order to be able to perform the same optimization process than the one made in Excel. A python script could be written to do so. It could automatically choose whether the round or square model have to be used and then make a loop on the staggering types and the weld size.

4.4 Conclusion

In final conclusion we can say that this subject implied to link several theory from structure to welding passing by programming. A gain in weight, price and time could be expect with the tool and especially if the FE model is successfully implement using the previous recommendations. Unfortunately the FE model was not validated but using some model modifications as provided above could allow verifying and validating this model and so the Excel results.

ACKNOWLEDGEMENTS

The author would like to thanks STX France and STX Solution for their help during my stay in Saint Nazaire. The author would like to thanks especially Adeline Vincent and Pierre-Yves L'Emeillat and the entire Hull department for sharing their knowledge.

The author would also like to thank EMShip professors and especially teacher from West Pomeranian University of Technology in Szczecin and Jean David Caprace who took the time to answer few questions about welding modeling.

This thesis was developed in the frame of the European Master Course in "Integrated Advanced Ship Design" named "EMSHIP" for "European Education in Advanced Ship Design", Ref.: 159652-1-2009-1-BE-ERA MUNDUS-EMMC.

REFERENCES

The author would like to point at that the majority of the documents used during this thesis are STX intern documents.

Design standards:

-*Construction principles of pillars continuity*, REV C, 2012

-*Definition of a pillar*, REV B, 2001

-*Metallic structure elements welds*, REV D, 2011

Classification society's rules

- *BV: Structure scantlings- Critical stress of pillar, Part 2 – Section 4-57 (January 1990)*

- *DNV: Stiffeners and pillars, Part 3 – Ch. 1 – Sec. 14*

- *LLOYD'S REGISTER: Pillars, Part 4 – Ch. 1 – Table 4 - 7*

-John Higgins, *HPC Best Practices for FEA, http://www.ansys.com/staticassets/ANSYS/Conference/Confidence/Boston/Downloads/hpc-best-practices-for-fea.pdf*

- Gene Poole, ANSYS Solvers Team, April, 2002

ANSYS equation solvers: usage and guidelines

APPENDIXES

A1 Diffusion Surface Without Reinforcement in Compression © STX

Confidential

A2 Zoom on Oblique Weld © STX

Confidential

A3 Diffusion Surfaces in Compression With Oblique Reinforcements © STX

Confidential

A4 Bending Calculation Using Old Method © STX

Confidential

A5 APDL Code

Confidential

A6 Additional Bibliography

As said on the main part of the report, classification societies provides us with several criteria for structure design. In our case, Bureau VERITAS provides us with the criteria available in Part B, Chapter 7 section 3 “primary supporting member”.

The general theory of the stiffened panel and the beam could also be used. In a more general manner, the beam theory and especially the beam buckling theory could perfectly suit the pillars calculation.

The author also found lectures, intern standards and books dealing about welding theory in general.

Some research papers were also found dealing with automatization and optimization.

Jean-David Caprace, Frederic Bair, Philippe Rigo. *Multi-criteria Scantling Optimization of Cruise Ships*, Ship Technology Research. Liège: University of Liège

A research paper (draft) on a numerical tool for the optimization of the scantlings of a ship considering production cost, weight and moment of inertia in the objective function. This tools verify VERITAS rules.

The following is a book about general shipbuilding, the section about pillars and welding are of our particular interest.
D. J. Eyres. *Ship Construction. Fifth edition*.M.Sc. F.R.I.N.A.

- Dr. Alan J. Brown, Dr. Wayne Neu, Dr. Owen Hughes, May 2005, *Tools for Multi-Objective and Multi-Disciplinary Optimization in Naval Ship Design*, Blacksburg, Virginia

- Tetsuya Yao, October 30, 2012, *Buckling/Plastic Collapse Behaviour and Strength of Ship Structures*

- Hyunyul Kim, *2004, Multi-Objective Optimization for Ship Hull Form Design*, Master of Science, Pusan National University

- A.-A.I ginnis, R. Duvigneauy, C. Politisz, K. Kostasz,K. Belibassakis, T. Gerostathisz and P.d. Kaklis , *A multi-objective optimization environment for ship-hull design based on a bem-isogeometric solver*.

- Dr. Alan Brown and LT Corey Kerns, *Multi-Objective Optimization in Naval Ship Concept Design*

- J. Jelovica & A. Klanac, *Multi-objective optimization of ship structures: using guided search vs., conventional concurrent optimization*

Helsinki University of Technology, Department of Applied Mechanics, Marine Technology, PL5300, 02015
TKK, Finland

- PhD thesis of Qiaofeng Chen, *Ultimate strength of stiffened panels steel and aluminium ship structures*, NTNU, Norway
Distributed to EMSHIP STUDENTS (2011-2012)

A7 Project Planning

During the project, the first two weeks were used to make a review of the work previously done in intern. After, implementation of the existing Excel macro using visual basic language was done in order to make the generalization of the process. This induced to include on the programming and the computation the various types of column junction with the structure and the various type of pillars (square, round…). Then the following weeks were used to make the link between this code and ANSYS software. The final stage of this work could be to implement an optimization loop allowing designer to quickly update the global model after modification.

Master thesis

Tâches

Nom	Date de début	Date de fin
Preliminary research	01/07/14	14/07/14
Review of previous work	02/07/14	10/07/14
Meeting with the engineering team	04/07/14	04/07/14
Study of BV rules	07/07/14	09/07/14
Visual Basic review	10/07/14	16/07/14
Integration of various pillars types	17/07/14	23/07/14
Meeting Eng II	17/07/14	17/07/14
Break time (Hollidays)	24/07/14	15/08/14
Generalization of the model	18/08/14	29/08/14
Meeting Eng III	08/08/14	08/08/14
Implementation of FEM	29/08/14	18/09/14
Statistics analyze	18/08/14	22/08/14
Results comparison and testing	19/09/14	30/09/14
Standardisation	18/08/14	04/09/14
Meeting Eng IV	01/09/14	01/09/14
Parametric design tool for pillars	01/10/14	14/10/14
Redaction of master thesis	07/10/14	20/10/14
Review of master Thesis	21/10/14	31/10/14
Meeting Eng V	23/09/14	23/09/14
Registration in Poland	24/09/14	30/09/14

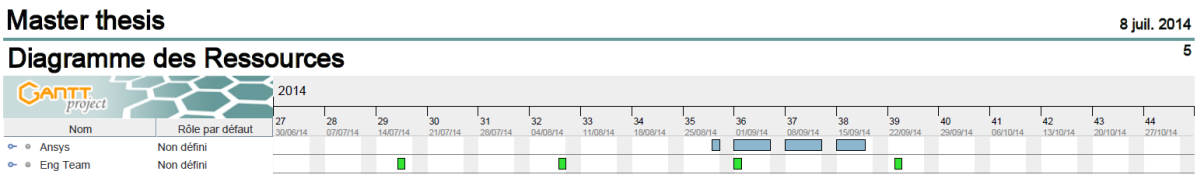

Diagramme de Gantt

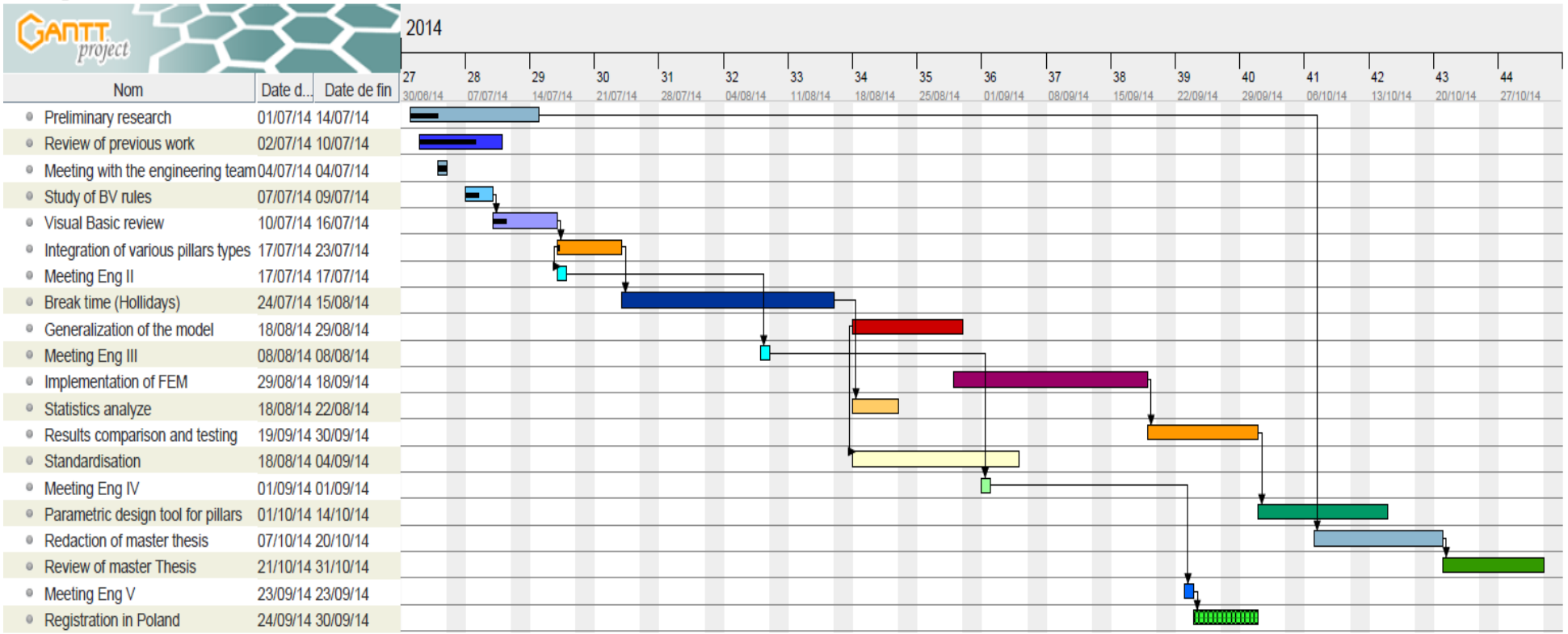

Nom	Date d...	Date de fin
Preliminary research	01/07/14	14/07/14
Review of previous work	02/07/14	10/07/14
Meeting with the engineering team	04/07/14	04/07/14
Study of BV rules	07/07/14	09/07/14
Visual Basic review	10/07/14	16/07/14
Integration of various pillars types	17/07/14	23/07/14
Meeting Eng II	17/07/14	17/07/14
Break time (Hollidays)	24/07/14	15/08/14
Generalization of the model	18/08/14	29/08/14
Meeting Eng III	08/08/14	08/08/14
Implementation of FEM	29/08/14	18/09/14
Statistics analyze	18/08/14	22/08/14
Results comparison and testing	19/09/14	30/09/14
Standardisation	18/08/14	04/09/14
Meeting Eng IV	01/09/14	01/09/14
Parametric design tool for pillars	01/10/14	14/10/14
Redaction of master thesis	07/10/14	20/10/14
Review of master Thesis	21/10/14	31/10/14
Meeting Eng V	23/09/14	23/09/14
Registration in Poland	24/09/14	30/09/14

A8 Manual Results

Confidential

A9 Node Selection

Confidential

A 10 Others FE Simulation

On the following, some of the most significant simulation results are displayed. This additional simulations were made in order to try to match the laboratory results especially in constraint.

Table 11: FE results for linear behavior element for 2 oblique

FEM results for pillar number four with a number of 50970 linear elements without morphing			
Loading [KN]	**Deformation X min [mm]**	**Deformation X max [mm]**	**Deformation total [mm]**
0	**0**	**0**	**0**
50	-1.08E-01	1.28E+00	1.40E+00
60	**-1.36E-01**	**1.59E+00**	**1.73E+00**
70	-1.59E+00	1.85E+00	2.02E+00
80	**-1.81E-01**	**2.12E+00**	**2.30E+00**
90	-2.04E-01	2.38E+00	2.59E+00
100	**-2.27E-01**	**2.65E+00**	**2.88E+00**

Intermediate Constraint min [Pa]	**Intermediate Constraint max [Pa]**	**Von Mises constrainte min [Pa]**	**Von Mises constrainte max [Pa]**
0	**0**	**0**	**0**
-3.82E+08	1.23E+09	4.71E+05	3.46E+09
-4.78E+08	**1.54E+09**	**5.88E+05**	**4.32E+09**
-5.58E+08	1.80E+09	5.04E+09	5.04E+09
-6.38E+08	**2.06E+09**	**7.95E+05**	**5.76E+09**
-7.17E+08	2.31E+09	8.83E+05	6.48E+09
-7.97E+08	**2.57E+09**	**9.82E+05**	**7.20E+09**

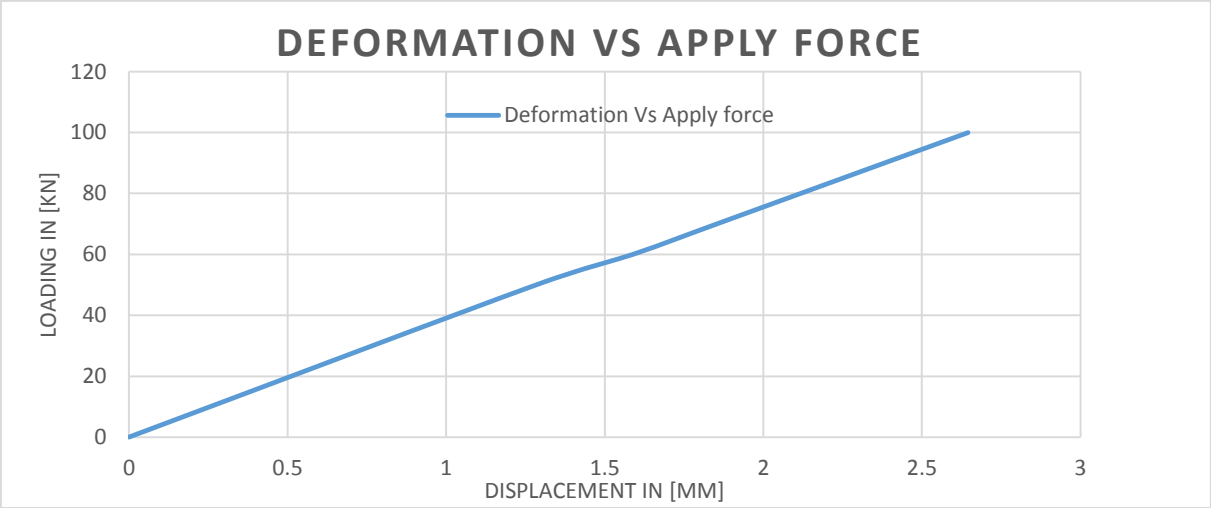

Figure 71: Deformation VS apply load

Table 12: Study of the influence of big displacement on 2 oblique symmetric model

	SYM without big displacements	SYM with big displacements
Load [KN]	Maximum displacement along X [mm]	Maximum displacement along X [mm]
0	0	0
50	2.5055	2.5363
60	3.0045	
70	3.5034	3.5676
80	4.0022	
90	4.5011	
100	4.9998	5.1461
120		
150		7.8871

A11 Results of Laboratory Tests

Confidential

A12 Diagram of the Program's Working